Limits of Perception:
Advances in Bio-Imaging

A Physiological Society Residential Topic Meeting

Monday 8 – Thursday 11 August 2016

University of Warwick, UK

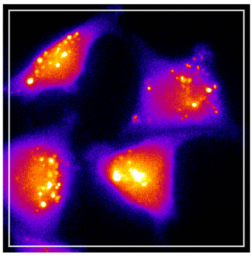
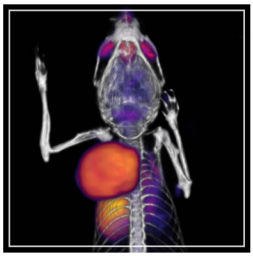
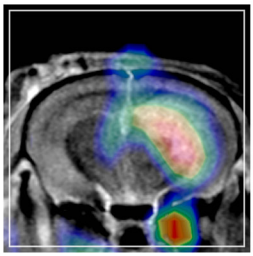
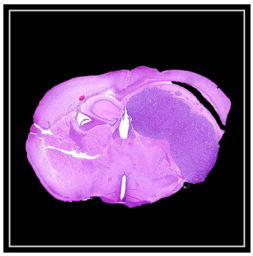

Scientific programme organisers

Mark Lythgoe, Daniel Stuckey & Tim Witney

Centre for Advanced Biomedical Imaging

University College London, UK

The Physiological Society



Physiology Friday!

Friday 14 October

Join us in celebrating Physiology Friday by spreading your love for your discipline through outreach and public engagement activities.

Hold an open day in your lab, put on an exhibition, organise a public lecture or debate, visit schools or local community groups, bake a cake, write a poem, start a social media campaign, do all you can to spread your passion for the science of life.

Email **outreach@physoc.org** to find out about partnership and funding opportunities.

biology week

#PhysiologyFriday
www.PhysiologyFriday.org

The Physiological Society

Contents

The Physiological Society Fourth Topic Meeting
Limits of Perception: Advances in Bio-Imaging
A Physiological Society Residential Topic Meeting

Organised by Mark Lythgoe, Daniel Stuckey & Tim Witney, Centre for Advanced Biomedical Imaging, University College London, UK

Monday 8 – Thursday 11 August 2016

University of Warwick, Warwickshire, Coventry, CV4 7AL

nanoScan® SPECT/MRI

nanoScan® PET/MRI

nanoScan® SPECT/CT

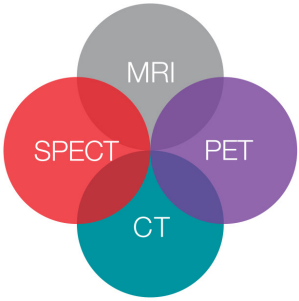

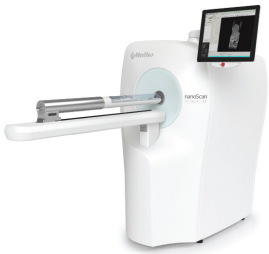

nanoScan® PET/MRI 3T

nanoScan® SPECT/CT/PET

nanoScan® PET/CT

bartec

Mediso

Welcome to what we hope will be a fascinating and highly interactive meeting that explores the interface of imaging science and physiology, 'Limits of Perception: Advances in Bio-Imaging'.

We are delighted to be here at the University of Warwick, and hope that you enjoy the variety of scientific and social meetings and activities taking place over the next few days.

When The Physiological Society approached us to guide them in organising a Topic Meeting, we were excited by the challenge to bring together many of the world's leading imaging researchers. Our aim is to kindle discussion and future collaboration across all scales of physiology and imaging, from the microscopic, through to the whole organism and into the clinic. We are delighted to have been able to attract such a broad range of truly leading international scientists to speak about the next generation of imaging tools.

The success of a meeting is not built around the speakers or the programme, but relies on the audience. Now it's up to all of us to make this meeting a success; to learn, challenge and interact with scientists from different disciplines, and hopefully build relationships that can change imaging science in physiology. But above all, let's have some fun, enjoy some exciting science and make some new friends.

We look forward to welcoming you to a great Residential Meeting, in Warwick.

Mark Lythgoe, Daniel Stuckey and Tim Witney
Scientific programme organisers

The Physiological Society, through its programme of scientific meetings, aims to support scientists in the United Kingdom, Europe and the Rest of the World to communicate their latest research to peers, policymakers and funding bodies. These meetings are recognised for their high quality and impact on scientific discovery. The Society hosts an annual conference, Physiology, in the summer.

BRUKER

Multimodality Molecular Imaging

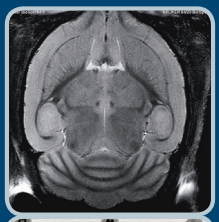

MRI
MPI*

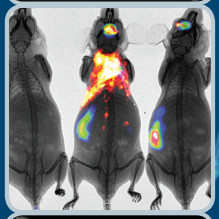

Fluorescence
Luminescence
Radioisotopic

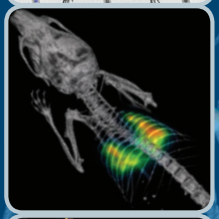

PET
SPECT
CT

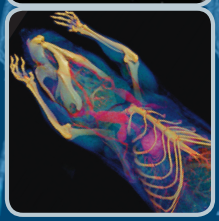

High Resolution
microCT

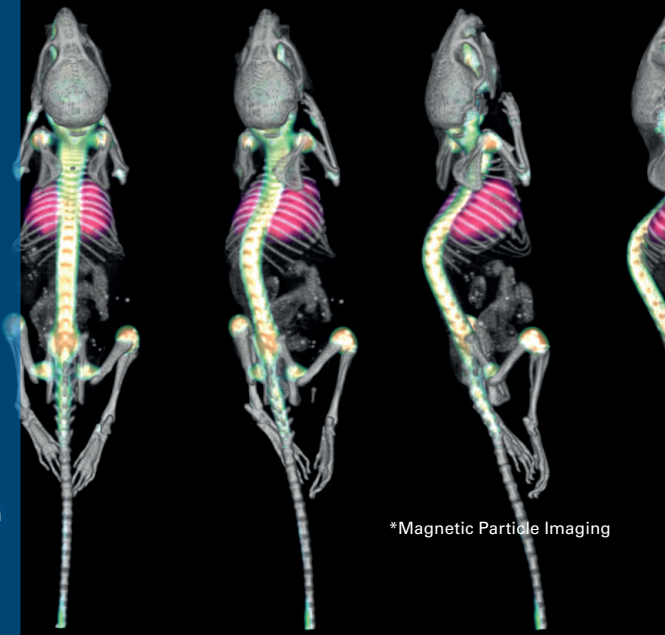

*Magnetic Particle Imaging

Nine Imaging Modalities, Unlimited Research Capabilities

Cutting-edge technology for disease research, translational science and molecular imaging. Trust our expansive portfolio of market-leading multimodal technologies to power your research success.

www.bruker.com/preclinicalimaging

Innovation with Integrity

Monday 8 August

17.00	Arrival, registration and check-in
18.00	Welcome and Introduction Mark Lythgoe, University College London, UK
18.15	Introductions from invited speakers
19.00	Alternative imaging approaches Jimmy Bell, University of Westminster, UK
19.45	Dinner and networking Rootes Restaurant, Rootes Building

Tuesday 9 August

8.00 Breakfast
Rootes Restaurant, Rootes Building

9.20 Introduction to day one
Daniel Stuckey, University College London, UK

Imaging Technology
Sponsored by Trasis
Radiopharmacy Instruments

TRASIS
RADIOPHARMACY
INSTRUMENTS

9.30 Shedding light on the human brain: The use of near infrared spectroscopy to monitor cerebral oxygenation, haemodynamics and metabolism
S06 Clare Elwell, University College London, UK

10.10 Imaging molecular dynamics in mouse cancer models
S13 Kurt Anderson, the Francis Crick Institute, UK

10.50 OME's OMERO & Bio-Formats: Open tools for image data and metadata access scale
S08 Jason Swedlow, University of Dundee, UK

11.30 Refreshments

Oral communications

12.00 An activatable contrast agent for photoacoustic imaging to probe oxidative stress in cancer
C06 Judith Weber, University of Cambridge, UK

12.10 Multimodal *in vivo* imaging of CAR T cell therapies of brain malignancies
C17 Tammy Kalber, University College London, UK

12.20 Evaluation of the ligand [18F]IMA201 as a novel radiotracer for aggregated alpha-synuclein in Parkinson's disease
C10 Erica Smyth, Imanova Ltd, UK

12.30 3D electron tomography analysis of cardiomyocyte ultrastructure
C02 Eva Rog-Zielinska, Imperial College London, UK

12.40 Visualisation of caspase activity using fluorescence lifetime optical projection tomography in live zebrafish
C13 Natalie Andrews, Imperial College London, UK

12.50 125I-FITI, an isatin-derived caspase-3 selective SPECT tracer for quantifying cell death in experimental myocardial infarction
C01 Daniel Stuckey, University College London, UK

13.00 Lunch

Imaging Probes/Reporters

14.00 Probes for transient molecular targets: Reactive oxygen species, DNA damage, and cell death
S01 Adam Shuhendler, University of Ottawa, Canada

Tuesday 9 August

14.40 PET/MRI: Multiparametric Iimaging in preclinical and translational research
S10 Bernd Pichler, University of Tubingen, Germany

15.20 Insertable, implantable and wearable micro-optical devices for the early detection of cancer
S09 Christopher Contag, Stanford University, USA

16.00 Refreshments

16.20 Poster pitches (three minute presentations) followed by poster viewing, refreshments and networking

Monitoring liver fibrosis disease progression and resolution with cell therapy
C14 John Connell, University College London, UK

Novel multi-modal imaging agent for stem cell tracking
C16 May Zaw Thin, University College London, UK

Longitudinal *in vivo* evaluation of colorectal tumour response to liposomal butyrate therapy using bioluminescence imaging
C09 Ana Gomez Ramirex, University College London, UK

Magnetic Resonance Imaging (MRI) reveals multiple facets of gastric motor function in Ehlers-Danlos Syndrome (hypermobility-type)
C11 Heather Fitzke, University College London/Queen Mary University of London, UK

C21 Non-invasively assessing the microstructural changes in tissue post-fixation using VERDICT MRI
Ben Jordan, University College London, UK

C07 Intracardiac administration for cell delivery to the kidneys and multi-modal cell tracking
Lauren Scarfe, University of Liverpool, UK

C05 Exploring visual network connectivity in mice using DCM fMRI
Arun Niranjan, University College London, UK

C20 Assessment of radiation damaged mouse lungs using perfluorohexane liquid MRI
Alexandr Khrapichev, CR-UK/MRC Oxford Institute for Radiation Oncology, UK

Alternative Imaging Approaches

18.45 Einstein's brain
Mark Lythgoe, University College London, UK

19.30 Dinner and networking
BBQ, Piazza, Rootes Building

Wednesday 10 August

8.00 Breakfast
Rootes Restaurant, Rootes Building

9.20 Introduction to day two
Tim Witney, University College London, UK

Multi-Modal Imaging Across Scales
Sponsored by Trasis Radiopharmacy Instruments

9.30 Multi-scale computational anatomy for image guided interventions
S11 David Hawkes, University College London, UK

10.10 The Iron Age
Po-Wah So, King's College London, UK

10.50 Refreshment break

Oral Communications

11.30 MRI characterisation of iron overload in a humanised mouse model of β-thalassemia major
C19 Laurence Jackson, University College London, UK

11.40 Developing cardiac PET tracers to hit hypoxia where it hurts
C08 Richard Southworth, King's College London, UK

11.50 X-ray excitation of CdTe quantum dots
C15 Sean Ryan, University of Hertfordshire, UK

12.00 Multi-modal multi-scale whole-body *in vivo* imaging to track spontaneous cancer metastasis and treatment response
C12 Alessia Volpe, King's College London, UK

12.10 PET imaging of tumor glycolysis downstream of hexokinase through noninvasive measurement of pyruvate kinase M2
C18 Tim Witney, University College London, UK

12.20 Super-oscillatory polarisation contrast for super-resolution imaging of unlabelled cells
C03 Edward Rogers, University of Southampton, UK

12.30 Lunch

Translational Imaging

13.30 Leveraging spontaneous disease in pets to develop advance imaging
S02 Dara Kraitchman, Johns Hopkins University, USA

14.10 How imaging pain, analgesia and altered states of consciousness gives us insights into human perception
S05 Irene Tracey, University of Oxford, UK

14.40 Tractometry and the limits of Microstructural Imaging
S12 Derek Jones, Cardiff University, UK

15.30 Refreshments

Wednesday 10 August

Molecular Imaging

16.00 Naked to the bone: Biomedical imaging at UCL
Mark Lythgoe, University College London, UK

16.40 Molecular imaging and theranostics of cancer
S07 Zaver Bhujwalla, Johns Hopkins University, USA

17.20 Posters, refreshments and networking

19.30 Conference Dinner
Panorama Suite, Rootes Building

Workshops – Limits of Bioimaging: lessons from the past and the future of imaging

Which imaging techniques/modalities/experiments held so much promise, but delivered so little; and how can we use this to inform the future of imaging?

8.00	Breakfast Rootes Restaurant, Rootes Building
9.00	Introduction to workshops - split into three groups
9.10	Compile a list of imaging related disciplines/projects/ methods that have NOT lived up to expectation Pick the top two to present to the group, with reasoning
10.00	Break
10.10	Compile a list of imaging related disciplines of the future Pick the one to present to the group, with reasoning and suggested pathway to realisation.
10.50	Break and refreshments
11.00	Reports from workshops
13.15	Prizes and concluding remarks
13.30	Lunch and close of meeting

Speaker Biographies

Kurt I. Anderson is a cell biologist with a long-standing interest in light microscopy.

Following his doctoral work on actin dynamics in cell migration with Vic Small at the Institute for Molecular Biology in Salzburg, he completed a short post-doc with Rob Cross at the Marie Curie Cancer Research Institute (Oxted) examining the adhesion dynamics of fish keratocytes. Dr. Anderson then moved to the newly formed Max Planck Institute for Molecular Cell Biology and Genetics in Dresden, where he set up the light microscopy facility.

In Dresden he continued to work on actin dynamics, and demonstrated in 2005 that the leading edge is a lipid diffusion barrier. The same year he was recruited to the Beatson Institute in Glasgow, where he has pioneered the use of advanced fluorescence imaging techniques such as FRAP and FLIM-FRET to study the molecular dynamics of disease and response to therapy in pre-clinical cancer models.

In 2012 he was the first recipient of the Royal Microscopical Society Life Sciences Medal for outstanding achievements applying microscopy in the field of cell biology.

Earlier this year he moved to the Francis Crick Institute, where he leads the Crick Advanced Light Microscopy Facility (CALM).

Zaver Bhujwalla is a Professor in the Departments of Radiology and Oncology at the Johns Hopkins University School of Medicine.

Dr. Bhujwalla's work is dedicated to the applications of molecular imaging to understand and target cancer and the tumor microenvironment.

Dr. Bhujwalla is a Fellow of the International Society of Magnetic Resonance in Medicine, the American Institute of Biomedical Engineers, and the World Molecular Imaging Society.

At the Johns Hopkins University School of Medicine she serves as Director of the Division of Cancer Imaging Research, the JHU ICMIC Program, and the MRB Molecular Imaging Center and Cancer Functional Imaging Core.

She co-directs the Cancer Molecular and Functional Imaging Program of the Sidney Kimmel Comprehensive Cancer Center.

Dr. Bhujwalla serves as Chair of the Career Development Advisory Committee of the Department of Radiology.

Speaker Biographies

Clare Elwell is a Professor of Medical Physics in the Department of Medical Physics and Biomedical Engineering at University College London (UCL).

She obtained her BSc. in Physics with Medical Physics in 1988 from the University of Exeter, where she also completed her MPhil (1991). She gained a PhD from UCL in 1995 describing the application of near infrared spectroscopy to measurements of brain oxygenation and blood flow in adults.

She now leads the Near Infrared Spectroscopy Research Group in the Biomedical Optics Research Laboratory at UCL and holds honorary positions at University College London Hospital, the National Hospital for Neurology and Neurosurgery, University of Essex and Birkbeck, University of London.

She develops novel optical systems for monitoring and imaging the human body. Her research projects include studies of autism, acute brain injury in adults, children and infants, sports performance, migraine and malaria. Her most recent project is the use of near infrared spectroscopy to investigate malnutrition related brain development in rural Gambia, resulting in the first functional brain imaging of infants in Africa.

Her research is supported by the EPSRC, MRC, Wellcome Trust, Bill and Melinda Gates Foundation and industrial collaborators Hamamatsu Photonics and Hitachi Medical Systems.

She is a founder member and President Elect of the Society for Functional Near Infrared Spectroscopy.

Derek Jones studied physics at Nottingham, before training as a medical physicist and ultimately undertaking a PhD in diffusion tensor MRI.

Postdoc positions took him to the Institute of Psychiatry in London and the National Institutes of Health, before moving to Cardiff in 2006 to establish the Cardiff University Brain Research Imaging Centre (CUBRIC).

A decade later, he is Director of the newly expanded CUBRIC – one of the largest neuroimaging research centres in Europe – (officially opened on 7 June).

The Centre houses 4 MRI scanners, MEG, brain stimulation, cognitive testing and sleep laboratories.

He holds an Investigator Award from the Wellcome Trust and is Fellow of the ISMRM, and Royal Society of Biology.

Speaker Biographies

Dara Kraitchman, VMD, PhD, FACC is a Professor of Radiology and Molecular and Comparative Pathobiology at The Johns Hopkins University School of Medicine. She is currently the Cardiovascular and Interventional Section Head in the Division of MR Research. She received her Bachelor's of Science degree in Electrical Engineering (BSEE) from Carnegie-Mellon University. After working in integrated circuit design at Bell Laboratories, she returned to academia and completed her Masters in Bioengineering, PhD in Bioengineering, and Doctorate of Veterinary Medicine at the University of Pennsylvania. As a veterinarian and bioengineer, she devoted her early career to developing non-invasive methods with magnetic resonance imaging (MRI) to study cardiac mechanics and perfusion.

Her group was the first to demonstrate non-invasive delivery and tracking by MR, radionuclide, and X-ray imaging of stem cells for cardiac regenerative therapy in a relevant large animal model. Recently, she has developed a novel method to protect mismatched stem cells from immunodestruction and enable tracking with non-invasive imaging. She has published over 100 peer-reviewed papers, is on the editorial board of Journal of the American College of Cardiology CV Imaging and Journal for Cardiovascular Magnetic Resonance Imaging, and has been continuously funded by the National Institutes of Health since 1989. She is a fellow of the International Society for Magnetic Resonance in Medicine and the American College of Cardiology.

She is also the Director of the Center for Image-Guided Animal Therapy, which is the first center in an academic medical institution to perform diagnostic imaging and minimally invasive techniques in client-owned pets with naturally occurring disease, as a means to develop more advanced therapies for pets and humans.

Bernd Pichler is Head of the Department of Preclinical Imaging and Radiopharmacy, Clinic of Radiology, University of Tübingen, Germany. Dr. Pichler studied electrical engineering with a focus on biomedical engineering and cybernetics at the Technical University of Munich.

He finished his diploma thesis in 1997 at the Max-Planck-Institute for Physics, Munich and the Department of Nuclear Medicine, Technical University of Munich, in the field of detector development for small animal positron emission tomography. He earned his PhD in physics at the Department of Nuclear Medicine, Technical University of Munich, in 2002 and subsequently worked as Assistant Biomedical Research Engineer (Assistant Research Professor) in the laboratory of Prof. Dr. Simon Cherry at the Department of Biomedical Engineering, University of California, Davis, USA, for two years.

Since 2005 he is head of the Laboratory for Preclinical Imaging and Imaging Technology at the Department of Radiology, University of Tübingen, and received the venia legendi (habilitation in experimental radiology) from the Eberhard Karls University of Tübingen in 2007. In December 2007, Dr. Pichler accepted the call of the University of Tübingen for a full (W3) professorship in "Preclinical Imaging and Imaging Technology".

In 2008 he became head of the Radiopharmacy and in 2011 both, the Laboratory for Preclinical Imaging and the Radiopharmacy joined, to become the Department of Preclinical Imaging and Radiopharmacy with Prof. Pichler as head of the department.

Speaker Biographies

Adam Shuhendler completed his undergraduate training at the University of Toronto, studying Forensic Sciences and Toxicology. He continued to a Masters in Pharmaceutical Sciences in Toronto, studying biochemical toxicology of drug-drug interactions to enhance cancer chemotherapy.

This work fed into his Doctorate in the same department, developing nanoparticle dosage forms for drug delivery to multidrug resistant breast cancer. In efforts to track the fate of his nanoparticles, he developed an interest in imaging that led him to a postdoc at Stanford University in the Molecular Imaging Program.

There, Adam developed skills in enzyme and bioanalyte-sensitive molecular imaging agent design and implementation. In July 2015, Adam took up an assistant professorship in the Dept of Chemistry and Biomolecular Sciences at the University of Ottawa.

His lab focuses on the development of MRI and PET molecular imaging agents that report on the activity of enzymes and small molecules with biochemical importance in cancer, atherosclerosis, and inflammation.

Irene Tracey holds the Nuffield Chair of Anaesthetic Science and is Head of the Nuffield Division of Anaesthetics and is Associate Head of the Medical Sciences Division/School at the University of Oxford, England.

Irene did her undergraduate and graduate studies at the University of Oxford and held a postdoctoral position at Harvard Medical School. Over the past 16 years her multidisciplinary research team has contributed to a better understanding of pain perception, pain relief and nociceptive processing within the injured and non-injured human CNS using neuroimaging techniques.

More recently, they have been investigating the neural bases of altered states of consciousness during anaesthesia. In 1998, Irene helped to co-found the now world-leading Oxford Centre for Functional Magnetic Resonance Imaging of the Brain (FMRIB) – the centre integrates research into key neurological and neuroscientific problems with cutting-edge developments in MR physics and data analysis (http://www.fmrib.ox.ac.uk).

The Centre has approximately 110 scientists and clinicians from a range of backgrounds and Irene was its Director from 2005 until 2015.

She has been appointed the new Head of the Nuffield Department of Clinical Neurosciences – a 450 person strong department comprising the FMRIB Centre, Division of Neurology, Nuffield Division Anaesthetics, Nuffield Laboratory Opthalmology and the Division for Prevention of Stroke and Dementia. She will take up that post in September 2016.

Speaker Biographies

Irene has served and continues to serve on many national and international committees, including the International Association for the Study of Pain as an elected Councillor until 2014 (Chair of the Scientific Program Committee for the Milan 2012 biannual world congress), Deputy Chair of the MRC's Neuroscience and Mental Health Board until 2014, the REF 2014 Psychology, Psychiatry and Neuroscience panel until 2014, and is co-Chair of the Canadian CERC panel and a member of the Brain Prize selection committee.

In 2008 she was awarded the triennial Patrick Wall Medal from the Royal College of Anaesthetists and in 2009 was made an FRCA for her contributions to the discipline. In 2015 she was elected a Fellow of the Academy of Medical Sciences. Irene is married to Professor Myles Allen, a climate physicist, and they have three wonderfully irrepressible children: Colette (18), John (14) and Jim (10).

HUMAN HEALTH

ENVIRONMENTAL HEALTH

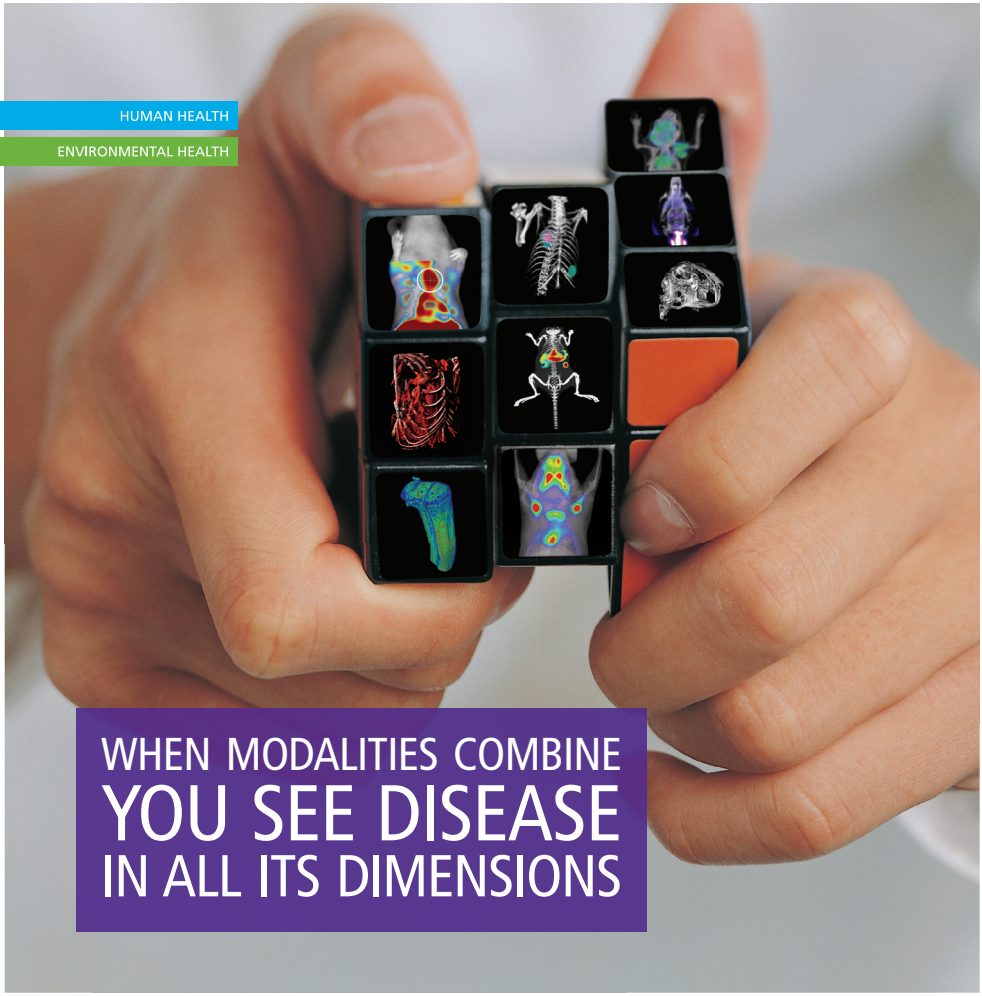

WHEN MODALITIES COMBINE YOU SEE DISEASE IN ALL ITS DIMENSIONS

It's simple: You need to glean more information from every *in vivo* experiment, giving you maximum data to enhance and broaden your biological understanding. And that's what's behind our multimodality imaging solutions. Coregistration is enabled through a combination of comprehensive optical, PET, and microCT platforms, plus a unique portfolio of bioluminescent cell lines and fluorescent agents. Together, these technologies offer a more complete visual assessment and understanding of disease treatment and progression over time, along with improved outcomes and treatment efficacy. Because when modalities combine, you see disease from *every* angle.

For research use only. Not for use in diagnostic procedures.

Visit our booth to learn more.

www.perkinelmer.com/Multimodality-Imaging

PerkinElmer®

For the Better

Copyright © 2016 PerkinElmer, Inc. 400318_11 All rights reserved. PerkinElmer® is a registered trademark of PerkinElmer, Inc. All other trademarks are the property of their respective owners.

Bartec Technologies

Bartec specialises in the supply, delivery, installation and support of Nuclear Medicine equipment and accessories.

Bartec has represented Mediso since 2002 for both clinical and pre-clinical imaging systems.

Mediso's technology platform includes positron emission, nuclear medicine, X-ray computer tomographic and magnetic resonance technologies. We offer the nanoScan® in vivo preclinical small animal imagers and MultiScan® in vivo translational imagers for molecular imaging, including the PET, SPECT, X-ray CT and MRI modalities. MultiCell® small-animal environment systems are available to provide support and monitoring functions to laboratory animals during the preparation stage and the imaging process. We provide clinical and molecular research imaging instrumentation for nuclear medicine applications.

Our products and support services are offered to universities, research hospitals, government agencies, pharmaceutical companies and contract research organizations in the UK and Globally.
In addition to partnering Mediso - Bartec has a vast portfolio and currently represents the following Manufacturers in the UK: Biodex Medical Systems for Nuclear Medicine Accessories, ec2 Solutions for RMIS/NMIS, ITD for Dedicated Radiopharmacy Furniture, Hoy Shielding, Gilligan Engineering for Transportation systems, Data Spectrum Corporation for Imaging Phantoms and Eckert & Ziegler for Calibration sources.

Bruker

Bruker continues to build upon its extensive range of products and solutions, its broad base of installed systems and a strong reputation among its customers.

Being one of the world's leading analytical instrumentation companies, Bruker is strongly committed to further fully meet its customers' needs as well as to continue to develop state-of-the-art technologies and innovative solutions for today's analytical questions.

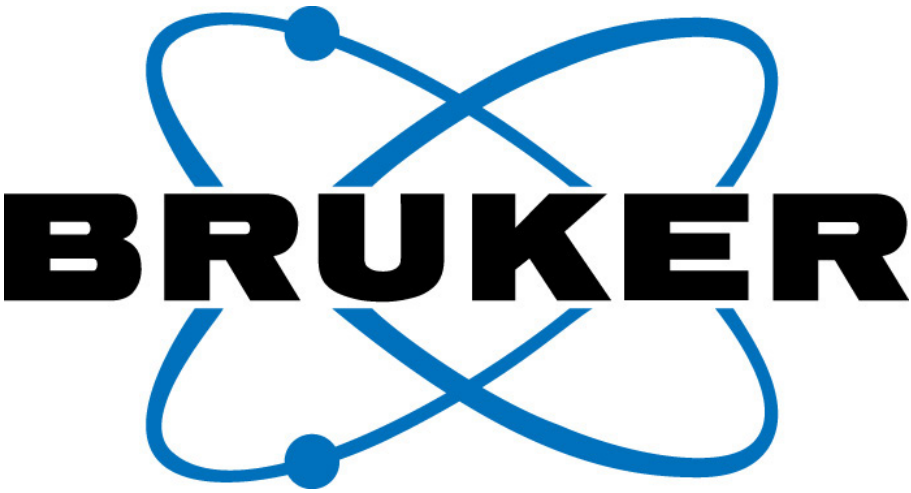

Imaging Equipment Ltd

Imaging Equipment Limited (IEL) is proud to be a distributor of international medical equipment for medical physics environments, including radiotherapy physics, diagnostic radiology, nuclear medicine, radiopharmaceuticals, radiation safety and radiation protection products. IEL represents 35 manufacturers and specialises in the effective use of radiation in medicine for both diagnostic and therapeutic purposes, and its successful relationships with manufacturers is based on the sharing of customer feedback and joint commitment to good customer service. IEL has developed a strong reputation for bringing innovative products to the UK and Ireland and helping customers make the best use of their equipment.
Imaging Equipment Limited (IEL) is the largest independent distributor of specialist Nuclear Medicine products in the UK and Ireland and offers a wide portfolio of products including Radiopharmaceuticals, PET injectors, Radionuclide Therapy, Shielding and Radiation protection.

Imaging Equipment Limited (IEL) is extremely proud to be representing such global market leaders in the Nuclear Medicine arena as; Advanced Accelerator Applications (AAA)*, Cyclomedica, Eckert and Ziegler, ROTOP and Tema Sinergie, thus being able to accurately match customers' requirements and build packages that meet both their technical specifications and budgetary demands.

IEL's team of specialist Nuclear Medicine sales consultants, supported by a dedicated and experienced technical team, provide a personal and high-quality customer service across the UK and Ireland.
*Imaging Equipment Limited is owned by Advanced Accelerator Applications PLC (AAA) of Geneva, Switzerland NASDAQ: AAAP

PerkinElmer is a global leader focused on improving human and environmental health, for the better.

To accelerate the understanding of human health, we provide our customers with the knowledge, expertise and solutions to better diagnose, treat and prevent disease.

Our innovative and integrated detection, imaging, software, reagents and services solutions are accelerating discovery in core areas of research including epigenetics, genomics, cellular research, quantitative pathology, in vivo imaging, biotherapeutics and informatics.

For more information visit www.perkinelmer.com/lifescience

PerkinElmer®
For the Better

Trasis

Trasis is a leader in the development and manufacturing of high quality instruments and consumables dedicated to radiopharmacy.

Its products currently include radio-synthesizers, dispensers, injection systems and shielding solutions. The company also provides custom synthesis development services.

Its experience has indicated that the merge of the mechanical design, software and chemistry skills is the key factor of success in our field. Trasis offers the expertise of this multidisciplinary team to support your production and development projects.

TRASIS

RADIOPHARMACY
INSTRUMENTS

General Information
The Physiological Society team can always be found at the registration desk. We will be happy to help with any queries you may have but you might be able to find an answer to your question on these pages.

Registration
The registration desk is situated on the in the Sciences Buildingwill be open at the following times:

Monday 8 August	17.00 – 19.00
Tuesday 9 August	8.30 – 18.30
Wednesday 10 August	8.30 – 18.00
Thursday 11 August	8.30 – 12.00

Poster help desk
This is at the registration desk. You can find Velcro to affix your poster here. No other fixings may be used. You can also find out when you are scheduled to present.

Internet access
There is free Wi-Fi on campus, and in accommodation via the "Warwick Guest" Wi-Fi network.

Mobile phones
Don't forget to turn off your mobile during all sessions at the meeting.

Video or audio recording of presentations
Attendees are reminded that the video and audio recording of ANY session or presentation using mobile devices or any such recording equipment is strictly prohibited.

Changes to abstracts
We cannot make changes to abstracts.

Smoking
You can't smoke inside in the UK. If you wish to smoke then you need to go to the designated smoking area.

Arriving late to sessions
We know it is not always possible to get to sessions on time but we do ask that if you are running late, to take your seat quietly.

Food and drink
All refreshments are included in your registration at times detailed in the programme.

Certificate of attendance
If you need a certificate of attendance and haven't already requested one, please ask at the registration desk or email events@physoc.org.

Twitter
The official Twitter hashtag is #bioimaging. Make sure you are following @ThePhySoc to keep up to date on what's happening at the event.

Feedback
We want you to enjoy this meeting but are always happy to hear how we can improve. You can speak to a member of the team, or fill in your comments anonymously in a feedback questionnaire that will be emailed to you after the meeting.

In case of emergency
The Physiological Society team are your first point of contact in any emergency. They will help you or find the person who can.

S01

Probes for transient molecular targets: Reactive oxygen species, DNA damage, and cell death

A. Shuhendler[1,3,2]

[1]*Chemistry and Biomolecular Sciences, University of Ottawa, Ottawa, ON, Canada,* [2]*University of Ottawa Brain and Mind Research Institute, Ottawa, ON, Canada and* [3]*University of Ottawa Heart Institute, Ottawa, ON, Canada*

The outward manifestation of our physiology in health or disease is the culmination of an array of sub-cellular events driven by molecular machines. These machines range from large enzymes to reactive small molecules, all of which exert an effect on the cell to alter its function for better or for worse. These active biomolecules rarely work in isolation, but are rather parts of integral networks within which any single sub-cellular machine is only transiently active or transiently present, giving way to its successor in the signaling chain. This transiency often renders these biomolecular machines elusive to analysis in the context of the living organism. Measuring the activity of these molecules and overcoming the difficulty of target transiency can enable both the detection of disease prior to outward signs and symptoms, and the assessment of the success or failure of therapy prior to disease progression. Molecular imaging is a powerful tool for assessing a target biomolecular machine non-invasively and longitudinally over an entire volume of interest in living subjects. New chemistries for activatable molecular imaging probes and the implementation of these probes in living animals will be described, focusing on the detection of three transient biomolecular machines turned on early in subcellular signaling cascades. *Reactive oxygen species (ROS)* are highly reactive oxygen-centered biomolecules underlying a broad range of diseases. In the context of injury, ROS are very early effectors of the tissue response to the source of harm. Novel optical nanoprobes have been developed from semiconducting polymers that can sensitively report on the presence of specific ROS in living mice [1,2]. The application of these nanoprobes to the real-time detection of the very early response to sterile tissue injury, as well as the real-time assay of drug-induced hepatotoxicity in living animals will be discussed. This nanoprobe enables ROS assays *in vivo* that were previously confined to the *in vitro* space. *Poly (ADP ribose) polymerase-1/2 (PARP-1/2)* is an enzyme that monitors DNA integrity, where PARP-1/2 activity acts as an intracellular signal selecting between DNA repair or cell death. PARP enzymes catalyze the polymerization of nicotinamide adenine dinucleotide (NAD), a transient polymer product that can be degraded within minutes of its formation by specific glycohydrolases. The development of a substrate-based radiotracer for the mapping of PARP-1/2 activity by positron emission tomography (PET) will be discussed, as well as its implementation in animal models of radiation therapy against breast or cervical cancer [3]. PARP-1/2 activation was detected hours after low dose radiation therapy, as was enzyme inhibition following PARP inhibitor therapy. This unprecedented *in vivo* investigation of

PARP-1/2 revealed differences in the timing of therapy response between tumor types, suggesting that timing of interventions are tumor type-specific. *Caspase-3* is a cysteine-aspartate protease whose activation signals the committal of the cell to die through apoptosis, a common death pathway induced by a variety of cancer chemotherapeutics and radiation. A modular probe was designed to undergo bio-orthogonal macrocyclization upon activation by caspase-3, with the macrocycles self-assembling into nanoparticles *in situ* in tumor tissue [4,5,6,7]. Since caspase-3 activity correlated with the degree of probe retention in dying tumor tissue, this molecular imaging strategy was applicable to optical, PET, and magnetic resonance imaging (MRI). This self-assembling molecular imaging probe was able to detect apoptosis induced by doxorubicin or radiation therapy in tumor-bearing mice following systemic administration of contrast agent. Enhanced contrast production following therapy was not detected using a non-activatable control analog, illustrating the utility of our bioorthogonal self-assembly probe design for therapy response monitoring. In discussing these three transient biomolecular machines as targets of molecular imaging, a variety of probe chemistries will be introduced and the ability to obtain non-invasive, longitudinal, and predictive data about sub-cellular physiology within the intact organism will be demonstrated. The molecular imaging of these key sub-cellular machines is sure to continue to provide an unprecedented level of interrogation of physiology to both enhance our investigations of health and disease, and improve clinical outcomes.

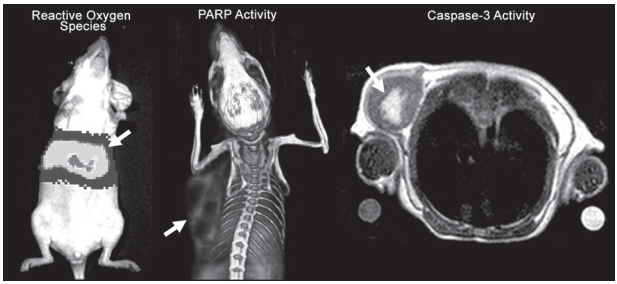

Transient biomolecular machines underly key sub-cellular functions that appear very early in the onset of disease or therapeutic response. The non-invasive, longitudinal detection of the activity of these biomolecular machines is difficult, but new probe chemistries across a range of modalities have made these targets accessible. The imaging of transient biomolecular targets including ROS in injury (far left), and the activity of PARP-1/2 (middle) or caspase-3 (far right) in response to cancer therapy will be discussed.

Pu K, Shuhendler AJ, et al (2013). *Angew. Chem. Int. Ed.* **23**, 10325-10329

Shuhendler AJ, et al (2014). *Nature Biotech.* **32**, 373-380

Shuhendler AJ, et al (2015) US Utility Patent 14/974,447

Ye D, Shuhendler AJ, et al. (2014). *Nature Chem.* **6**, 519-526

Ye D, Shuhendler AJ et al. (2014). *Chemical Sci.* **4**, 3845-3852

Shuhendler AJ, et al. (2015). *Scientific Reports* **5**, 14759

Shen B, et al. (2013). *Angew. Chem. Int. Ed.* **52**, 10511-10514

I gratefully acknowledge the work of Prof. Kanyi Pu, Prof. Deju Ye, Prof. Lina Cui, and Prof. Kim Brewer who all made key contributions to this body of work. Funding for this work was graciously provided by the Susan G. Komen Foundation, Stanford Cancer Institute Translational Research Award, National Cancer Institute CCNE and ICMIC, DoD BCRP. The Natural Science and Engineering Research Council of Canada, the Canadian Foundation for Innovation, and the Canada Research Chairs program are also acknowledged as current funders.

Where applicable, the authors confirm that the experiments described here conform with the Physiological Society ethical requirements.

S02

Leveraging spontaneous disease in pets to develop advance imaging

D.L. Kraitchman[1,2,3]

[1]Radiology, Johns Hopkins University, Baltimore, MD, USA, [2]Center for Image-Guided Animal Therapy, Johns Hopkins University, Baltimore, MD, USA and [3]Molecular and Comparative Pathobiology, Johns Hopkins University, Baltimore, MD, USA

At present, approximately one in two households owns a pet with about quarter of these pets being dogs or cats. Due to the high degree of inbreeding in domestic dogs and cats, over 350 of the diseases in pets also occur in human patients. Unlike transgenic mice where specific genes are knocked in or knocked out to cause disease, the genetic mutations in dogs and cats that leads to naturally occurring diseases may not be elucidated. However, naturally occurring diseases in pets offers several advantages over purpose bred animals for probing physiology. In particular, pets with naturally occurring diseases often have many of the underlying co-morbidities seen in human patients, are treated with a variety of medications, and experience varying environments that in turn alter genetic expression of disease.

For imaging applications, dogs and cats are sufficiently large enough to use clinical imaging equipment and pediatric or adult devices with little to no modifications. In particular, more than 50% of dogs >10 years of age will develop malignancies. For example, osteosarcoma (OSA) is the most common bone tumor in dogs and has many similarities to human OSA.(1) An example of MRI-guided cryotherapy of a bone tumor is show in Fig 1. While ischemic heart disease and thromboembolic disease are relatively rare in pets without underlying renal disease and neoplasia, many other forms and risk factors of cardiovascular disease, such as diabetes mellitus (2), mitral valve disease (3), and dilated cardiomyopathy (4), are prevalent in pets. Diseases showing similarities to neurological diseases in man, such as multiple sclerosis, Alzheimer's (5), and spinal cord injury, are also prevalent in pets. Examples of potential stem cell and drug therapy targets and monitoring with imaging will be presented.

Clinical trials in pets must often undergo similar regulatory processes for device and drug approval and ethical review, which may vary by local regulatory bodies. In some cases, preclinical data in research animals may be neccessary to perform clinical trials in pets, which is similar to tradition drug and device development for translation to human studies. However, the use of spontaneous disease in pets may be not only informative for human clinical trials but also provide new therapies for treatment of diseases in domestic animals.

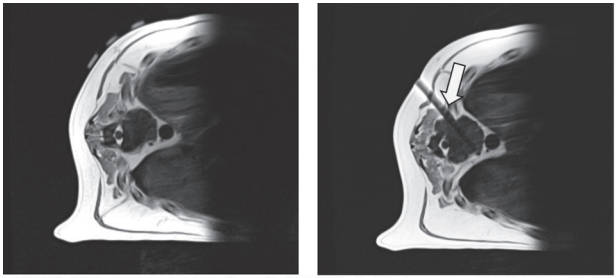

Left: Axial MRI of a boney lesion in the vertebral body of a large breed dog. Right: MRI-compatible biopsy device (arrow) appears as a hypo-intensity on proton density MRI. Using MRI guidance, the lesion can be targeted while avoiding critical nervous and venous structures. This spontaneous disease in dogs can potentially be used for targeted therapies. Adapted from Krimins *et al.*

Withrow SJ, Powers BE, Straw RC & Wilkins RM. (1991). Comparative aspects of osteosarcoma. Dog versus man. *Clinical orthopaedics and related research*, 159-168.

Krimins RA, Fritz J, Gainsburg L, Gavin P, Ihms EA, Huso DL & Kraitchman DL. (in press). MR-Guided Bone Biopsy of a T11 Vertebral Body Mass in a Rottweiler. *J Am Vet Med Assoc*.

Davison LJ, Herrtage ME & Catchpole B. (2005). Study of 253 dogs in the United Kingdom with diabetes mellitus. *Vet Rec* **156,** 467-471.

Garncarz M, Parzeniecka-Jaworska M, Jank M & Loj M. (2013). A retrospective study of clinical signs and epidemiology of chronic valve disease in a group of 207 Dachshunds in Poland. *Acta veterinaria Scandinavica* **55,** 52.

Calvert CA, Pickus CW, Jacobs GJ & Brown J. (1997). Signalment, survival, and prognostic factors in Doberman pinschers with end-stage cardiomyopathy. *J Vet Intern Med* **11,** 323-326.

Head E, McCleary R, Hahn FF, Milgram NW & Cotman CW. (2000). Region-specific age at onset of beta-amyloid in dogs. *Neurobiology of aging* **21,** 89-96.

This work is supported in part by the National Institutes of Health (R01-EB017615 and R33 HL0089029), the Maryland Stem Cell Research Foundation, (2011-MSCRFIII0043 and 2015-MSCRFE-1891), the Johns Hopkins Discovery Award, and private donations supporting the Center for Image-Guided Animal Therapy.

Where applicable, the authors confirm that the experiments described here conform with the Physiological Society ethical requirements.

S05

How imaging pain, analgesia and altered states of consciousness gives us insights into human perception

Irene Tracey, University of Oxford, UK

For the past 18 years, we have used multimodal imaging approaches to understand human pain. Pain, as a highly subjective perceptual experience, does not only have significant clinical relevance but is an important gateway into understanding human perception. Manipulating the experience with pharmacological agents, cognitive, mood and context manipulations provide additional means by which we can get a more causal understanding of the neural basis of perception. Finally, our recent work using multimodal imaging to understand the neural basis of anaesthesia-induced altered states of consciousness provides us with additional opportunities to understand human perception. In my talk, I will provide examples from all these areas of our work.

S06

Shedding Light on the Human Brain: the use of near infrared spectroscopy to monitor cerebral oxygenation, haemodynamics and meta

Clare Elwell, University College London, UK

Near infrared spectroscopy (NIRS) has found widespread application as an optical monitoring and imaging technology for the assessment of cerebral oxygenation, haemodynamics and metabolism. The technique relies upon the relative transparency of biological tissue to light in the near infrared part of the spectrum allowing the measurement of changes in concentration of chromophores such as oxy and deoxyhaemoglobin. The continuous, non invasive and bedside nature of the measurement has led to a wide range of applications in the clinical and life sciences. Our group at UCL have developed a suite of NIRS monitoring and imaging systems employing broadband, frequency domain and time resolved spectroscopy techniques optimized for studies in newborns, young infants, children and adults. We have also developed novel spectroscopy methods for the measurement of oxidation status of cytochrome c oxidase as a marker of cerebral cellular oxygen metabolism[1]. Many of these techniques are being used to investigate acute brain injury in clinical settings, specifically on adult and neonatal intensive care. The possibility of acquiring trend measures of haemodynamic variables at high temporal resolution has prompted renewed interest in the use of optical techniques to assess cerebral autoregulation and vasoreactivity in a range of patient groups with specific interest in charting the dynamics of autoregulatory processes in the injured brain[2]. Mathematical models of cerebral blood flow and metabolism have been developed to aid interpretation of these multimodal clinical datasets[3].

The use of NIRS trend measures to map the haemodynamic response to neuronal activation, so called functional near infrared spectroscopy (fNIRS), is well established. There has been particularly interest in the use of fNIRS to investigate typical and atypical neurodevelopment in young infants in whom the choice of neuroimaging modalities is severely restricted. In collaboration with the Centre for Brain and Cognitive Development, Birkbeck, University of London, we have shown the potential of fNIRS to provide an early predictive marker of autism in infants as young as four months of age[4]. Furthermore the technology is well placed for applications in resource poor settings and we have recently established the GlobalfNIRS initiative (www.globalfnirs.org) to support the use of fNIRS in global health projects worldwide. As part of this initiative, and with funds from the Bill and Melinda Gates Foundation, we have proved the efficacy of fNIRS measures of brain function in Gambian infants over the first two years of life, resulting in the first functional brain imaging of infants in Africa[5]. We are now embarking on a longitudinal birth cohort study to deliver brain function for age curves in Gambian and UK infants to investigate the impact of early life risk factors, including undernutrition, on infant brain development.
This talk will describe the advances in instrumentation, data analysis and interpretation which have made these studies possible, and will look towards the future prospects for this application of the technology in the clinical and life sciences.

1. Bale G., Elwell C., Tachtsidis I. (2016) From Jöbsis to the present day: a review of clinical near-infrared spectroscopy measurements of cerebral cytochrome-c-oxidase J Biomed Opt. 21(9):91307
2. Highton D., Ghosh A., Tachtsidis I., Panovska-Griffiths J, Elwell CE, Smith M (2015) Monitoring cerebral autoregulation after brain injury: multimodal assessment of cerebral slow-wave oscillations using near-infrared spectroscopy. Anesth Analg.121(1):198-205
3. Banaji M, Mallet A, Elwell CE, Nicholls P, Cooper CE. (2008) A model of brain circulation and metabolism: NIRS signal changes during physiological challenges PLoS Comput Biol. Nov;4(11):e1000212
4. Lloyd-Fox, S., Blasi, A., Elwell, C. E,Charman, T., Murphy, D., Johnson, M. H. (2013). Reduced neural sensitivity to social stimuli in infants at risk for autism. Proc. Royal Soc B. Biol. Sci. 280(1758)
5. Lloyd-Fox, S., Papademetriou, M., Everdell, N. L., Darboe, M. K., Wegmuller, R., Prentice, A. M., Moore, S. E., Elwell, C. E. (2014). Functional near infrared spectroscopy (fNIRS) to assess cognitive function in infants in rural Africa. Scientific Reports 4:4740

S07

Molecular imaging and theranostics of cancer

Zaver M. Bhujwalla, The Johns Hopkins University School of Medicine, USA

The applications of noninvasive molecular and functional imaging in cancer can provide new insights in understanding cancer, by identifying new functional roles for genes and pathways, defining the role of stromal cells in tumor progression, and understanding the impact of abnormal physiological and metabolic environments on tumor growth, response to treatment, and metastasis, within the backdrop of the spatial and temporal heterogeneities that exist in tumors. With the availability of whole-body imaging, the impact of cancer on structural, functional, and molecular characterization of various organs can be investigated in a 'holistic' approach, especially for cancer-associated syndromes such as cachexia. Molecular and functional imaging also provide unique opportunities to develop theranostic strategies for precision medicine in cancer. Located at the interface of detection and therapy, the field of theranostics has resulted in a rapid expansion of innovative nanoplatforms that are being developed based on the imaging modality, the therapeutic cargo, and the target. There is an increasing trend to combine imaging modalities by decorating these nanoplatforms with multi-modal imaging reporters. Receptors and antigens expressed specifically by cancer cells provide the most direct targets for cancer-specific treatments. However, most cancers do not express specific receptors and antigens, creating a critical need to mine other aspects of the tumor such as metabolism, angiogenesis, inflammation, the tumor microenvironment (TME), and stromal cell receptors for theranostics. Physiological environments in tumors that are characterized by hypoxia, acidic extracellular pH, and substrate deprivation, and the TME that consists of the extracellular matrix (ECM), cancer associated fibroblasts (CAFs), adipocytes, pericytes, multiple immune cells such as tumor associated macrophages (TAMs), and vascular and lymphatic endothelial cells, also provide opportunities for theranostic imaging. The exciting opportunities in molecular, functional, and theranostic imaging that are occurring at the cross-section of chemistry, molecular biology, and imaging provide tangible hope in finding effective treatments against cancer.

S08

OME's OMERO & Bio-Formats: Open tools for image data and metadata access scale

Jason Swedlow, University of Dundee, UK

Despite significant advances in cell and tissue imaging instrumentation and analysis algorithms, major informatics challenges remain unsolved: file formats are proprietary, facilities to store, analyze and query numerical data or analysis results are not routinely available, integration of new algorithms into proprietary packages is difficult at best, and standards for sharing image data and results are lacking. We have developed an open-source software framework to address these limitations called the Open Microscopy Environment (http://openmicroscopy.org). OME has three components—an open data model for biological imaging, standardised file formats and software libraries for data file conversion and software tools for image data management and analysis.
The OME Data Model (http://openmicroscopy.org/site/support/ome-model/) provides a common specification for scientific image data and has recently been updated to more fully support fluorescence filter sets, the requirement for unique identifiers, screening experiments using multi well plates. The OME-TIFF file format (http://openmicroscopy.org/site/support/ome-model/ome-tiff) and the Bio-Formats file format library (http://openmicroscopy.org/site/products/bio-formats) are easy-to-use tools for converting data from proprietary file formats. These resources enable access to data by different processing and visualization applications, sharing of data between scientific collaborators and interoperability with third-party tools like Fiji/ImageJ. The Java-based OMERO platform (http://openmicroscopy.org/site/products/omero) includes server and client applications that combine an image metadata database, a binary image data repository and visualization and analysis by remote access. The current stable release of OMERO (OMERO 5.2; http://downloads.openmicroscopy.org) includes a single mechanism for accessing image data of all types-- regardless of original file format-- via Java, C/C++ and Python and a variety of applications and environments (e.g., ImageJ, Matlab and CellProfiler). OMERO includes SSL-based secure access, distributed compute facility, filesystem access for OMERO clients, and a scripting facility for image processing. An open script repository allows users to share scripts with one another. A permissions system controls access to data within OMERO and enables sharing of data with users in a specific group or even publishing of image data to the worldwide community. OMERO 5.0 includes updates and resources that specifically support large datasets that appear in digital pathology and high content screening. Importing these large datasets is fast, and data are stored in their original file format, so they can be accessed by 3rd party software. Several applications that use OMERO are now released by the OME Consortium, including FLIMfit, a fluorescence lifetime analysis module; u-track, an object tracking module; image-based search applications, OMERO.searcher and WND-CHARM; an automatic image

tagging application, a biobanking application (http://www.openmicroscopy.org/site/products/partner). OMERO and Bio-Formats run the JCB DataViewer (http://jcb-dataviewer.rupress.org/), The Image Data Repository (http://idr-demo.openmicroscopy.org) and are used to publish 3D EM tomograms in the EMDataBank (http://emdatabank.org/). They also power several large project image data repositories (e.g., http://lincs.hms.harvard.edu/; http://ssbd.qbic.riken.jp/;). All OME software is available at http://openmicroscopy.org.

Jason R. Swedlow[1],[2] and the OME Consortium[3]
[1]Centre for Gene Regulation & Expression, University of Dundee, Dundee, Scotland, UK.
[2]Glencoe Software, Inc. Seattle, WA, USA
[3]http://www.openmicroscopy.org/site/about/who-ome

S09

Insertable, implantable and wearable micro-optical devices for the early detection of cancer

Christopher Contag, Stanford University, USA

Current technologies for the detection of cancer lack the sensitivity for early detection at times when therapy would be most effective, and cannot detect minimal residual disease that persists after conventional therapies. At the same time there is a paradigm shift occurring in medicine moving to disease characterization based on molecular etiologies--this shift is leading to molecularly targeted imaging, diagnosis, and therapy and will lead to advances in molecularly-targeted prevention. Determining the molecular etiologies of cancer requires new technologies and more integrated approaches, which will in turn lead to early detection and more effective treatment. In the area of biomedical imaging, it will be necessary to develop image-guided approaches for multiplexed molecular characterization of cancer and methods to visualize small numbers of cancer initiating cells. Imaging and sensing will need to move from detection limits of 1 cm masses to 1 mm, or even 100 μm diameter masses, and new technologies with this sensitivity need to be developed. Optical imaging has the sensitivity for this level of detection and there are a number of recent advances that will enable the use of optics in the clinic for cancer detection. Optical imaging tools image over a range of scales from macro- to nanoscopic resolution and can provide molecular sensitivity and cellular level resolution. Developments in the field of optical imaging will be useful in informing diagnosis, prognosis and therapy, and for guiding biopsies for multiparameter molecular analyses. To meet these needs, molecular probes are being developed that are activated at the target site and can be used to reveal biomarkers of disease in situ. New instruments based on micro-optical designs can be used to reach in the body to reveal microanatomic and molecular detail that are indicators of early cancers. We are advancing the technologies that enable miniaturization of 3-D scanning confocal

microscopes to examine tissue in situ for early anatomic and molecular indicators of disease, in real time, and at cellular resolution. These new devices will lead to a shift from the current diagnostic paradigm of biopsy followed by histopathology and recommended therapy, to one of non-invasive point-of-care diagnosis with the possibility of treatment in the same session. By creating the tools for point-of-care pathology we are reducing the time and distance between the patient and the diagnostic event, and changing the practice of medicine. The emerging combinations of instruments and molecular probe strategies will reveal disease states in finer detail and provide greater information to clinicians for more informed, and directed therapies. Personalized medicine is really molecular medicine and the new imaging and diagnostic tools that characterize molecular basis of disease are driving personalized care and early intervention.

S10

PET/MRI: Multiparametric Imaging in Preclinical and Translational Research

Bernd Pichler, University of Tübingen, Germany

Combined PET/MRI technologies have matured over the last years and have found their places as emerging tools in preclinical and clinical research. Our aim is to exploit the potential of PET/MR in various fields of biomedical research focusing on imaging of immune cell trafficking, cancer research, neurodegeneration and infectious diseases. The wealth of multiparametric morphological, functional and molecular information provided by PET/MR requires advanced methods of image data analysis and data mining. One of our approaches is to combine in vivo imaging data with omics information which links imaging science and the powerful disciplines of omics and bioinformatics. The talk will also include the topic of immune cell trafficking.

S11

Multi-Scale Computational Anatomy for Image Guided Interventions

David Hawkes, University College London, UK

Abstract: This talk summarises projects and progress in active computational models applied to image guided interventions within the Centre for Medical Image Computing at UCL, London. A hierarchy of complexity of models is introduced covering locally rigid transformations, models that incorporate tissue motion, biomechanical properties, cross-population statistics of shape and deformation and multi-scale representations of shape ranging from whole organ down to cellular scale. Example applications are given in surgery for refractory epilepsy, laparoscopic surgery, radiotherapy of the lung, breast conserving surgery and the diagnosis and treatment of prostate cancer. Applications in laparoscopic surgery, prostate cancer interventions and epilepsy surgery have entered clinical trial and clinical translation of others are expected in the next five years.

S12

Tractometry and the limits of Microstructural Imaging

Derek Jones, Cardiff University, UK

In 1994, Basser and colleagues published a paper on how to estimate the diffusion tensor in tissue using MR-based techniques (J Magn Reson Ser B 103:247-254). This launched a whole new field of 'microstructural MRI', and a new focus on the white matter in the living brain – whether it is studying individual differences in the healthy brain, or group differences in neurological and psychiatric disorders.

The ubiquity of MRI pulse sequence and post-processing packages have made the performance of a white matter microstructure study widely accessible. While this has provided fresh insights into the role the white matter plays in normal and abnormal brain function, the most widely used tools / models can be considered 'blunt' at best.

This talk will explore the limitations of extant technologies, particularly with regard to interpretation of their output, before asking what properties of white matter we should be focusing on, and to what extent we can capture those properties non-invasively. Latest hardware for capturing properties such as axon diameter in vivo will be discussed, including the EPSRC-funded National Microstructural Imaging Facility, with 300 mT/m gradients, before finishing with open questions about where the limits of perception of white matter microstructure may lie.

S13

Imaging molecular dynamics in mouse cancer models

Max Nobis[1], Ewan McGhee[1], Anna-Karin E. Johnsson[2], Juliane P. Schwarz[1], Shereen Kadir[1], Jennifer P. Morton[1], Kevin B. Myant[1], David J. Huels[1], Douglas Strathdee[1], Karen Blyth[1], Owen J. Sansom[1], Heidi Welch[2], Paul Timpson[3], **Kurt I. Anderson**[1]

[1]The Beatson Institute for Cancer Research, Glasgow, UK
[2]Babraham Institute, Cambridge, UK
[3]The Garvan Institute, Sydney, Australia

Increasing progress has been made characterizing the genetic basis of human disease, however we must now strive to understand how genes drive disease progression and determine response to therapy. This requires that we study disease and therapeutic response in their native biological context, where microenvironmental parameters such as tissue stiffness, perfusion and hypoxia, and interactions among heterogeneous cellular populations are critical determinants of patient survival. In order to study cell signaling and adhesion in mouse cancer models at the molecular level, we have developed the use of two imaging approaches commonly used to study cellular biochemistry in vitro, FRAP and FRET. The approach we have developed is based on an experimental pipeline spanning

2D and 3D cell culture, organoids, ex vivo tissue imaging, transplantation models and full genetic models (Anderson et al., J Cell Sci 124:2877, 2012). Each of these experimental systems are optimal for acquiring different types of data, and provide complimentary information which ultimately informs and guides intravital imaging. We have also used abdominal imaging windows to perform longitudinal studies in the breast, intestine, and pancreas. I will summarize our experience on the use of FRET biosensors to study the activities of Rac (Johnsson et al., Cell Reports 6:1153, 2014) and Rho (unpublished) GTPases, and the use of FRAP to study cell adhesion (Erami et al., Cell Reports 14:152, 2016), in mouse cancer models. An emerging theme from our work is that we are able to quantify important differences in cell signaling and adhesion based on the location of cells within tumours, and proximity to blood vessels. Our data provide evidence for the microenvironmental influence on disease progression and response to therapy at the molecular level.

C01

^{125}I-FITI, an isatin-derived caspase-3 selective SPECT tracer for quantifying cell death in experimental myocardial infarction

D.J. Stuckey[1], A. Badar[1], M. Glaser[2], M. Zaw Thin[1], V. Taylor[1], V. Rajkumar[3], B. Pedley[3], T. Kalber[1], M.F. Lythgoe[1] and E. Arstad[2]

[1]Centre for Advanced Biomedical Imaging, UCL, London, UK, [2]Institute of Nuclear Medicine, UCL, London, UK and [3]Cancer Institute, UCL, London, UK

Myocardial cell death is implicit in heart disease and a major underlying cause of heart failure (1). Despite rapid advances in diagnostic technology there is still no reliable method for directly quantifying cardiac cell death *in vivo* (2). Here we report a novel isatin-derived ^{125}I-FITI SPECT radiotracer selective for the caspase-3 activity that underlies cell death.

Using ICMT-11 as a scaffold, ^{125}I-FITI was synthesised using a modified one-pot radiochemical reaction (3) with a bathophenanthroline catalyst (4). Myocardial infarction (40 min ischemia followed by reperfusion) was induced in 16 male C57Bl6 mice with 8 control mice undergoing sham surgery. Eighteen hours after surgery, cardiac function and viability were assessed in vivo using high frequency ultrasound and late gadolinium enhanced cardiac MRI (5). At 24 hours all animals underwent tail vein infusion of 0.5MBq of ^{125}I-FITI or a non-functional ^{125}I-FITI derivative. Animals were sacrificed after 15, 30, 60 and 120 minutes. Organs were collected and gamma counted for bio-distribution of tracer. Hearts immediately underwent sectioning, staining with cell viability dye TTC, followed by plating for autoradiography for high resolution ex vivo assessment of localisation of FITI within the infarcted hearts.

Ex vivo bio-distribution studies showed FITI uptake was highest in the stomach, thyroid, salivary glands and small intestine. Uptake of tracer within the hearts of control animals was low at all time points and reduced further by one and two hours after infusion. Ultrasound and MRI showed that all infarcted hearts had impaired contraction and small to medium infarct sizes of 17-38% (FIG). TTC staining concurred with this result (FIG). Autoradiographic assessment of radiotracer distribution within tissues showed high FITI accumulation within anterolateral regions of the myocardium (FigC). Comparison of FITI distribution with the in vivo MRI and in vitro TTC staining performed on the same hearts confirmed that these regions of tracer uptake corresponded with the location of the infarct. Importantly, the non-functional FITI derivative did not accumulate within the infarct region, indicating specificity of FITI binding. Sensitivity and specificity analysis confirmed accumulation of FITI within infarcted segments of the myocardium and that non-functional FITI had much lower sensitivity for myocardial cell death than the active compound. These data suggest that FITI accumulation is greatest at the site where cell death is maximal at 24 hours after myocardial infarction and that FITI is specifically binding the activated caspase3 present acuity after myocardial infarction. FITI may offer a novel imaging biomarker for quantification of cardiac cell death in vivo.

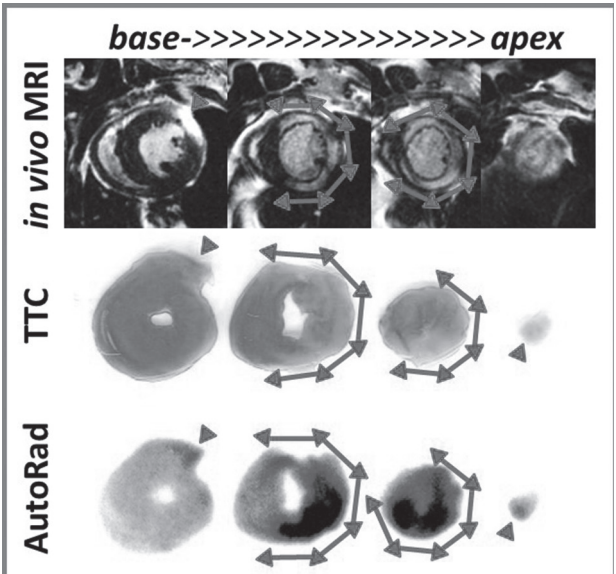

FIG: *Imaging cell death 24 hours after myocardial infarction*: LGE-MRI of infarct *in vivo*. TTC staining of infarct in tissue slices. Autoradiography of ^{125}I FITI accumulation within the infarcted regions of the myocardium (arrows)

L. R. Fiedler et al. Curr Top Dev Biol 2014, 109, 171

A. Niu et al. J Nucl Med 2010, 51, 1659

R. Yan et al., AngewChemIntEd 2011, 50, 6793, R. Yan et al. JACS 2013, 135, 703

H. S. Gill et al., JMedChem 2009, 52, 5816, L. Iddon et al., BioorgMedChemLett 2011, 21, 3122. E. Galante et al., Molecules 2013, 18, 5335

D. J. Stuckey et al Circulation Cardiovascular Imaging 2014, 7, 240

Where applicable, the authors confirm that the experiments described here conform with the Physiological Society ethical requirements.

C02

3D electron tomography analysis of cardiomyocyte ultrastructure

E. Rog-Zielinska[1], E. O'Toole[2], A. Hoenger[2] and P. Kohl[3,1]

[1]National Heart and Lung Institute, Imperial College London, Harefield, UK, [2]University of Colorado, Boulder, CO, USA and [3]Institute for Experimental Cardiovascular Medicine, University Heart Centre Freiburg / Bad Krozingen, Freiburg, Germany

Biological sciences in general have benefitted from rapid technology developments producing an ever-growing number of large, multidimensional data sets. In the context of structural imaging, this includes the move from 2D section-based insight to true 3D data collection. One of the most useful techniques allowing for exploration of cellular structures in 3D with unparalleled fidelity and nanometre resolution is electron tomography (ET).

In highly compartmentalised cells, such as cardiomyocytes, elaborate sub-cellular membrane structures play crucial roles in cellular electrophysiology and mechanics. Although the anatomy of specific ultra-structures, such as dyadic couplons, has been described using 2D electron microscopy (EM) of thin sections, we lack accurate quantitative knowledge of fine 3D spatial interrelations of other sub-cellular components. Here we illustrate the utility of 3D ET for identification, visualisation, and analysis of cardiac ultrastructures such as T-tubular system (T-tub).

Ventricular T-tub form an intricate system of surface membrane invaginations that, through their close connections with SR, support spatially and temporally synchronous excitation-contraction coupling throughout the cell. Due to their structural complexity and narrow lumen, T-tub enclose extracellular fluid, allowing for only restricted diffusional exchange with bulk extracellular contents. To explore whether T-tub deformation during the cardiac contraction-relaxation cycle may alter T-tub shape and volume-surface ratio, we conducted dual-axis 3D ET (voxel size 1.2nm) of ventricular tissue fragments of rabbit hearts (n=6), fixed in different mechanical states (contracture, cardioplegic arrest, volume load). We then determined T-tub cross-section, eccentricity (deviation from circular cross-section), and the angle between maximal T-tub radius (r_{max}) direction and Z-disc plane and analysed it as a function of sarcomere length. We found that, as SL increases, r_{max} orientation changes from near-parallel to Z-disks in contractured cells to near-perpendicular during maximal stretch ($P<0.001$). In parallel, a bi-phasic change in T-tub eccentricity was seen, with higher values at short and long SL, and lower levels in-between ($P<0.001$). Surprisingly, the extend of T-tub volume-surface ratio changes as a result of mechanical deformation was less than expected, possibly due to dynamic in-/excorporation of caveolae as a function of T-tub membrane tension.

Our findings show that T-tub undergo SL-dependent deformation, potentially associated with T-tub content mixing. Functional studies will investigate whether the changes in partial T-tub volumes could aid T-tub content exchange with the bulk extracellular space. We show that 3D ET yields accurate structural information that

provides a structural framework for mechanistic integration of molecular signalling networks.

Where applicable, the authors confirm that the experiments described here conform with the Physiological Society ethical requirements.

C03

Super-oscillatory polarisation contrast for super-resolution imaging of unlabelled cells

E.T. Rogers[2,1], S. Quraishe[4,2], T.A. Newman[4,2], J.E. Chad[3,2], N.I. Zheludev[1,5] and P.J. Smith[2,3]

[1]Optoelectronics Research Centre, Faculty of Physical Sciences and Engineering, University of Southampton, Southampton, UK, [2]Institute for Life Sciences, University of Southampton, Southampton, UK, [3]Biological Sciences, Faculty of Natural and Environmental Science, University of Southampton, Southampton, UK, [4]Clinical and Experimental Sciences, Faculty of Medicine, University of Southampton, Southampton, UK and [5]Centre for Disruptive Photonic Technologies, Nanyang Technological University, Singapore, Singapore

Super-resolution microscopy is opening up new avenues in the biosciences, however all widely-used techniques require addition of fluorescent probes. Now, we have demonstrated that optical-super-resolution imaging is possible in unlabelled living cells, using the phenomenon of optical super-oscillation.

Super-oscillation is an intriguing mathematical phenomenon, first described in the context of quantum mechanics. It is widely accepted that any function that is band-limited (in frequency) oscillates no faster (in time) than its fastest Fourier component. However, a band-limited super-oscillatory function may oscillate arbitrarily fast in regions of relatively low intensity [1]. In the context of optics, this means that we can create an arbitrarily small hotspot far from any lens or surface, simply using precisely engineered interference of light. Super-oscillatory hotspots, beyond the dark perimeter, are necessarily surrounded by sidebands that contain a significant fraction of the optical power – trading efficiency for resolution. To use this spot for imaging, we replace the conventional focusing lens in a confocal microscope with a super-oscillatory lens and use a confocal imaging arrangement to reject the light scattered from the sidebands. The resolution of the image formed is determined by the size of the super-oscillatory hotspot.

We previously demonstrated far-field imaging with sub-wavelength resolution on non-fluorescent manufactured samples [2]. We have developed the system further and can now image unlabelled cells at super-resolution. To do this we combine our super-oscillatory microscope with an advanced form of polarisation contrast imaging. The instrument is a modification of a standard confocal microscope, with two key components: spatial light modulators (SLMs) to shape the laser beam entering the microscope, and a liquid crystal (LC) panel to control the input polarisation. We

capture four different super-resolved images of the sample with different incident polarisations, from which we can calculate the anisotropy and orientation angle of each pixel (using a similar method to ref [3]). This highlights those parts of a cell with significant molecular structuring, such actin filaments, microtubules, and even protein enriched lipid bilayers such as vesicles and cell membranes.
We have applied this to cells, illustrated in figure 1, showing it is able to reveal new levels of information in biological samples. Figure 1a shows a schematic of our setup, and 1b shows a metal sector star sample illustrating the polarisation contrast, where brightness shows level of anisotropy and hue shows the polarisation angle at which most light is reflected. In c and d we show images of a live, unlabelled MG63 cell. The super-oscillatory image is sharper than the equivalent confocal image of the same system, seen even more clearly in the zoomed in insets i and ii.

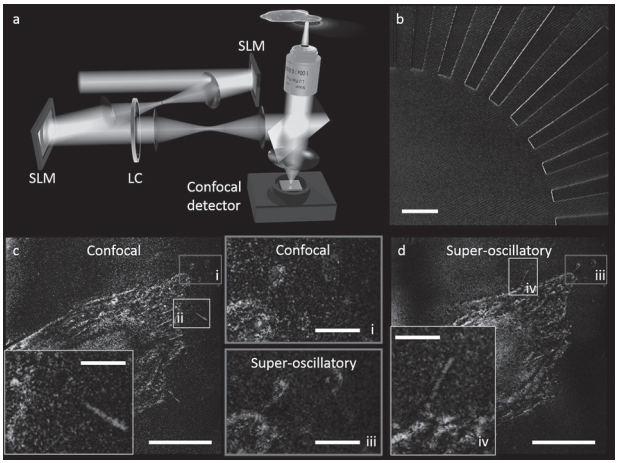

Super-oscillatory imaging system and results. a - Schematic of the setup (SLM - spatial light modulator, LC - Liquid crystal polarisation controller). b - Image of segment of a sector star showing gradual rotation of refelected polarisation as colour change. c,d - Confocal and super-oscillatory images of the same cell, 10 minutes apart. The super-oscillatory image shows sharper detail, which is most obvious in the insets. Scale bars in main figures are 10μm, in insets they are 2μm.

Berry, M. V & Popescu, S. Evolution of quantum superoscillations and optical superresolution without evanescent waves. *J. Phys. A. Math. Gen.* **39,** 6965–6977 (2006).

Rogers, E. T. F. *et al.* A super-oscillatory lens optical microscope for subwavelength imaging. *Nat. Mater.* **11,** 432–5 (2012).

Mehta, S. B., Shribak, M. & Oldenbourg, R. Polarized light imaging of birefringence and diattenuation at high resolution and high sensitivity. *J. Opt.* **15,** 094007 (2013).

Where applicable, the authors confirm that the experiments described here conform with the Physiological Society ethical requirements.

C04

Neurobehavioural activity of *Gongronema latifolium* in hypertensive rats model

J.A. Beshel[1,2]

[1]Department of Human Physiology, Cross River University of Technology, Calabar, Nigeria, Calabar, Nigeria and [2]Department of Human Physiology, University of Calabar, Calabar, Nigeria, Calabar, Nigeria

Hypertension, memory impairment, anxiety and locomotor disorders are all associated with ageing/old age. High salt feed is implicated in the etiology of hypertension. Over the years, salt (NaCl) is experimentally used to induce hypertension in rats. This study investigated the effect of *Gongronema latifolium,* a tropical plant with proven medicinal properties, on learning and memory, fear and anxiety, locomotor and exploratory behaviour in hypertensive rats' model. 28 Wistar rats assigned into 4 groups of 7 rats each were used for the study. Group 1 was given 0.9% normal saline as placebo. Group II, received 8% salt (NaCl) in feed, and 1% salt in drinking water. Groups III and IV, received same treatment as group II but was intervened with 200mg/kg and 400mg/kg extract of *Gongronema latifolium* respectively. Administration was via oral route and lasted for 42 days. All animals had access to food and drinking water *ad libitum*. The Morris water maze, light-dark transition box, and open field maze were used to assess learning and memory, fear and anxiety, locomotor and exploratory behaviour respectively. Ethical conscent was given. Results of the study showed a significant ($p<0.001$) dose-dependent decrease swimming latency in the extract treated groups compared with the salt-fed untreated group and the control, and a significant ($p<0.001$) lower swimming latency in the control group when compared with the salt-fed untreated group. The visible platform test also showed a significant ($p<0.001$) lower swimming latencies in the extract treated groups compared to the control and the salt-fed untreated groups. The swimming latencies in the salt-fed untreated group was however higher ($p<0.001$) when compared to the control. There was also, a significant dose dependent ($p<0.001$) increase in frequency of transitions, decrease stretch-attend posture, decrease grooming frequency and decrease dark-box duration in the extract treated groups when compared with the control and salt-fed untreated group. Yet, the salt-fed untreated group showed a significant ($p<0.001$) higher indices of stretch-attend posture, grooming frequency, dark-box duration, and increase transitions when compared with the control group. There was also a dose-dependent increase ($p<0.001$) line crossing activity, walling, rearing, and centre square entry in the extract treated groups compared with the control. These indices however, were found higher in the salt-fed untreated group compared with the control. These results put together suggests that extract of *Gongronema latifolium* increases visio-spatial learning and improves memory, decreases anxiety, and increases locomotor behaviour in a hypertensive rat model. Thus, if these results are applicable to humans, *Gongronema latifolium* could be used as a therapeutic

measure for the management of age-related complications of learning and memory, anxiety and locomotor disorders.

Edet EE, Akpanabiatu MI, Eno AE, Umoh IB, Itam EH (2009). Effect of Gongronema Latifolium crude leaf extract on some cardiac enzymes of alloxan-induced diabetic rats. *African Journal of Biochemical Research,* 3 (11): 366-369.

Bourin, M. and Hascoët, M. (2003). The mouse light/dark box test. *European Journal of Pharmacology*, 463, 55 – 65.

JA Beshel, RO Nneli, FN Beshel, CC Mfem and CO Nku (2014). Ethanolic root extract of *Carpolobia lutea* improves memory. Research & Reviews: *Journal of Medical and Health Sciences* Vol 3 (2) 86-90.

Where applicable, the authors confirm that the experiments described here conform with the Physiological Society ethical requirements.

C05

Exploring visual network connectivity in mice using DCM fMRI

A. Niranjan[1], P. Zeidman[2], J. Wells[1] and M.F. Lythgoe[1]

[1]Centre for Advanced Biomedical Imaging, University College London, London, UK and [2]Institute of Neurology, University College London, London, UK

Introduction: The visual pathway is an important neuroscience research target. In previous work [1], we characterised the BOLD response to visual stimulation in the mouse brain and modulated the BOLD response with respect to temporal frequency of visual stimulation [1]. Statistical parametric mapping successfully identified the lateral geniculate nuclei (LGd), the superior colliculus (SCs) and the primary visual cortex (VISp). However, standard mapping analysis provides no insight into casual mechanisms of visual processing. Dynamic causal modelling (DCM) [2] is an analysis technique that uses a Bayesian framework to compare models of effective connectivity between brain regions. There is limited use of DCM fMRI in the rat [3] and none in mouse. This work explores the use of DCM in healthy mice, and opens up the possibility of examining effective network connectivity in transgenic mice.

Methods: 8 female C57BL6/J mice weighing (20.7 ± 0.7) g were used. Medetomidine anaesthesia (0.4 mg/kg bolus, 0.8 mg/kg constant infusion) was used during functional imaging. Respiration was approximately (170 ± 20) breaths per minute, and core body temperature maintained at (37.0 ± 0.2) °C. Visual stimulation was conducted bilaterally with blue laser light (445 nm, Omicron). A block design was used (40 seconds of rest, 20 seconds of stimulus, 3 repeats per session). During stimulus blocks, the laser was pulsed at 1, 3, 5 or 10 Hz, with 10ms pulse duration. Subjects were scanned using a 9.4T MRI Scanner (Agilent Inc.). GE-EPI was used with 4 compressed segments.

Analysis: For each subject, all sessions of pre-processed EPI data were modelled using a general linear model, including regressors modelling the onset of optic

stimulation (S) and the parametric effect of stimulus temporal frequency (*f*). BOLD time series were extracted from LGd, SCs and VISp. DCMs were created for each subject, to explore which connections were modulated by *f* and which regions were driven by S. Connections between regions were considered to be bi-directional, and *f* was considered to either modulate nothing, LGd ↮VISp, SCs ↮VISp, or VISp itself. The driving effect of S was considered for all combinations of regions. In total this created a space of 168 models to be compared. A series of 3 random effects family model comparisons were conducted, with the model space partitioned into 'families' according to the question being addressed.

Results: There was evidence for a fully connected network (Fig.1A), with *f* modulating the LGd ↮VISp connection (Fig.1B), and S driving LGd and SCs (Fig.1C). These results are summarized by the network diagram in Fig.1D, which is consistent with studies tracing projections of retinal ganglion cells throughout the mouse brain [4]. We demonstrate the ability of DCM to make inferences of effective connectivity in the mouse brain which are consistent with tracer studies [4].

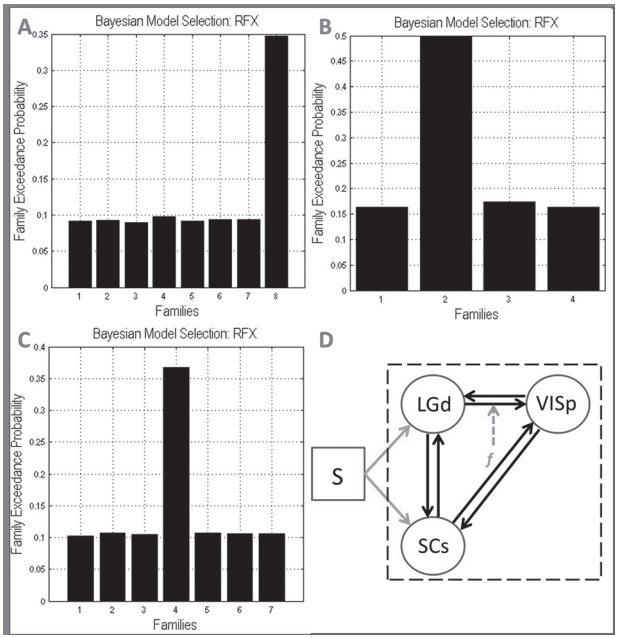

(A-C) RFX Bayesian model selection using family comparisons. A) Family 8 corresponds to fully connected models. B) Family 2 corresponds to *f* modulating LGd ↮VISp. C) Family 4 corresponds to models where the *S* drives LGd and SCs only. D) Network representation of results.

Niranjan A., et al. (under review)

Friston K.J., et al. 2003.

David, Olivier, et al. 2008.

Huberman, A.D., Niell, C.M., 2011.

UK MRC Grant (MR/K50077X/1)

Where applicable, the authors confirm that the experiments described here conform with the Physiological Society ethical requirements.

C06

An activatable contrast agent for photoacoustic imaging to probe oxidative stress in cancer

J. Weber[1,2], T. Zuehlsdorff[2], D. Cole[2], M. Di Antonio[1,3] and S. Bohndiek[1,2]

[1]Cancer Research UK Cambridge Institute, University of Cambridge, Cambridge, UK, [2]Department of Physics, University of Cambridge, Cambridge, UK and [3]Department of Chemistry, University of Cambridge, Cambridge, UK

Introduction: Photoacoustic imaging (PAI) is an emerging technique for the visualization of molecular processes *in vitro* and *in vivo*. PAI provides non-invasive images of the absorbed optical energy density at depths of several centimeters with a resolution of ~100 μm.(1) Cancer cells must survive both hypoxic and oxidative stresses as they proliferate to form a tumor mass. PAI is inherently sensitive to oxygen supply, and in turn hypoxic stress, based on endogenous contrast from oxy- and deoxy-hemoglobin.

We hypothesize that development of an activatable PAI probe responsive to hydrogen peroxide (H_2O_2) will enable simultaneous imaging of hypoxic and oxidative stress in tumors *in vivo* using PAI.

Methods: A near-infrared activatable contrast agent was synthesized based on: a heptamethine carbocyanine backbone(2); an H_2O_2 reactive unit(3),(4) connected via a linker unit; and glucose as a preliminary targeting moiety. Different linker structures between the backbone and H_2O_2 reactive unit were validated with regard to their ability to induce a change in the optical absorption spectrum of the dye. Optical and optoacoustic spectra were then examined under different environmental conditions (i.a. MeOH, H_2O, PBS ± FBS, plasma, ± H_2O_2). Expected interactions with MeOH and H_2O were predicted using density functional theory (DFT). As a first step towards *in vivo* application, optoacoustic imaging was then performed in tissue mimicking phantoms based on agarose gel containing intralipid and nigrosin black dye. First *in vitro* studies were performed using the HEK 293 cell line and modifying with concentrations of H_2O_2 ranging from 50 μM to 2 mM.

Results and Discussion: An activatable contrast agent was designed exhibiting an optical absorption peak at 730 nm (in H_2O), which shifted by 60 nm to 790 nm (in H_2O) after exposure to H_2O_2 (Fig. 1). Furthermore, the absorbance at 790 nm was found to increase by over 45%. The absorption spectrum was strongly dependent on the solvent, relating to polarity, hydrogen bonding capacity and ion content. The cause of the change in the absorption spectra was clarified by DFT, which showed conformational changes due to solvent interactions. For

optoacoustic imaging, the same trend was observed, although peaks were shifted by ~15 nm and broadened. Data acquired in phantoms show promise for future *in vivo* application.
Conclusion: We have synthesized the first activatable contrast agent for PAI that is based on a heptamethine carbocyanine dye and responsive to the presence of H_2O_2. In the future, we can target this approach using specific molecular markers expressed by cancer cells to study the presence of H_2O_2 under scenarios including therapeutic response. Future work could provide insight into the role of oxidative stress in cancer, inflammatory processes and other diseases.

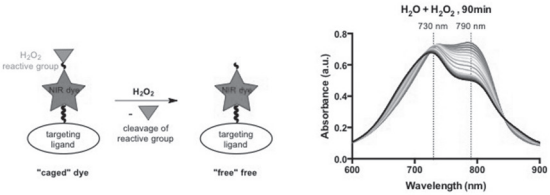

Reaction scheme of the near-infrared activatable probe with H_2O_2 and the correlated change in absorbance.

Beard P. Biomedical photoacoustic imaging. Interface Focus [Internet]. 2011;1(4): 602–31. Available from: http://www.pubmedcentral.nih.gov/articlerender.fcgi?artid=3262268&tool=pmcentrez&rendertype=abstract

Narayanan N, Patonay G. A New Method for the Synthesis of Heptamethine Cyanine Dyes: Synthesis of New Near-Infrared Fluorescent Labels. J Org Chem. 1995;60(17):2391–5.

Kim D, Kim G, Nam S-J, Yin J, Yoon J. Visualization of Endogenous and Exogenous Hydrogen Peroxide Using A Lysosome-Targetable Fluorescent Probe. Sci Rep [Internet]. 2015;5:8488. Available from: http://www.nature.com/doifinder/10.1038/srep08488

Kuang Y, Balakrishnan K, Gandhi V, Peng X. Hydrogen peroxide inducible DNA cross-linking agents: Targeted anticancer prodrugs. J Am Chem Soc. 2011;133(48):19278–81.

Where applicable, the authors confirm that the experiments described here conform with the Physiological Society ethical requirements.

C07

Intracardiac administration for cell delivery to the kidneys and multi-modal cell tracking

L. Scarfe[1,2], C. Astley[2], A. Taylor[1,2], P. Murray[1,2] and B. Wilm[1,2]

[1]Centre for Preclinical Imaging, University of Liverpool, Liverpool, UK and [2]Institute of Translational Medicine, University of Liverpool, Liverpool, UK

The most common route of cell administration in pre-clinical models is intravenous (IV)[1-2]. However, IV administration invariably results in cells becoming trapped in the lungs, and very few cells, if any at all, are able to escape the lungs[3]. We aimed to

optimise an ultrasound-guided intracardiac (US-IC) method of cell administration, in order to bypass the lungs and deliver cells to the kidney. The cells were tracked using two imaging modalities, bioluminescence imaging (BLI) and magnetic resonance imaging (MRI).

Female BALB/c severe combined immunodeficient (SCID) mice were administered 1 million mouse mesenchymal stem cells (mMSC) in 100μl via US-IC injection (*n=4*) or IV injection (*n=2*). mMSCs had been labelled with lentivirus-expressing luciferase for BLI, and with superparamagnetic iron oxide nanoparticles (SPIONS, ~8pg/cell) to enable MRI. Following subcutaneous injection of 150mg/kg luciferin, the mice were imaged with BLI, and subsequently with the 9.4T MR scanner (abdominal FLASH $T2^*$ scans). Mice were sacrificed immediately after imaging and organs were collected for *ex vivo* imaging and histology. An additional 3 mice were given US-IC injections and treated as described above, but re-imaged at 24h and 48h, and were sacrificed at 24h (*n=1*), or 48h (*n=2*).

US-IC administration of mMSCs led to a whole-body distribution of bioluminescence signal, compared with IV administration, which resulted in a signal limited to the lungs. MRI scans showed a darkening of the cortex of the kidneys of mice that received a US-IC injection, indicating the presence of SPION-labelled cells in this region. In the mice that received IV administration the kidneys were comparable to baseline. To determine for how long after administration SPION-labelled cells could be detected *in vivo*, mice were imaged at multiple time points after US-IC cell injection. In these animals, the cortex was much lighter by 24h, and by 48h the signal was close to baseline. This change in biodistribution over time was quantified by measuring the relaxation time within the cortex, which showed a significant decrease between baseline and the day of injection ($p < 0.001$), and a rise in relaxation time at 24h and 48h, which was not significantly different from baseline measurements (24h, $p = 0.133$; 48h, $p = 0.335$). This was consistent with BLI data, which showed a decrease in luciferase signal over time, and histological analysis of frozen kidney sections.

In conclusion, we have optimised a US-IC method of cell administration which results in successful delivery of cells to all organs of the body. With both BLI and MRI, we have successfully tracked SPION-labelled cells in the kidney, and showed that the cells were cleared from the kidney within 24h after administration.

Bussolati, B. *et al.* Isolation of Renal Progenitor Cells from Adult Human Kidney. Am. J. Pathol. **166**. 545-555 (2005)

Ronconi, E. *et al.* Regeneration of Glomerular Podocytes by Human Renal Progenitors. Am. J. Soc. Nephrol. **20**. 322-332 (2009)

Fisher, U. *et al.* Pulmonary Passage is a Major Obstacle for Intravenous Stem Cell Delivery: The Pulmonary First-Pass Effect. **18**. 683-691 (2009)

Where applicable, the authors confirm that the experiments described here conform with the Physiological Society ethical requirements.

C08

Developing cardiac PET tracers to hit hypoxia where it hurts

R. Southworth[1], R. Medina[1], F. Baark[1], E. Mariotti[1], M. Handley[1], J. Clark[2], T. Eykyn[1] and P. Blower[1]

[1]Imaging Sciences and Biomedical Engineering, King's College London, London, UK and [2]Cardiovascular Division, King's College London, London, UK

Rationale: The subtle hypoxia underlying chronic cardiovascular disease is an attractive target for PET imaging, but the lead hypoxia imaging agent ^{64}CuATSM, originally intended for cancer imaging, detects degrees of hypoxia far more extreme than would occur in the heart clinically. We are therefore developing analogs of ^{64}CuATSM better suited to identify compromised *but salvageable* myocardium at the point where it becomes vulnerable, identified and validated using parallel biomarkers of cardiac function, energetics and biochemistry comparable to those observed in cardiac patients.
Methods and Results: Isolated rat hearts (male Wistar 250g, n=6/group) were perfused with aerobic buffer for 20 min, then a range of hypoxic buffers (using a computer-controlled gas mixer) for 45 min. Contractility was monitored by intraventricular balloon, energetics by ^{31}P NMR spectroscopy, lactate and creatine kinase release spectrophotometrically, and HIF1α by Western blotting of tissue homogenates. We identified a key hypoxia threshold at 30% buffer O_2 saturation which induced a stable and potentially survivable functional and energetic compromise: LV developed pressure was depressed by 20%, and cardiac phosphocreatine was depleted by 65.5 ± 14% (mean +/- SD, $p<0.05$ vs control, ANOVA & t-test), but ATP levels were maintained. Lactate release was elevated (0.21 ± 0.067 versus 0.056 ± 0.01 mmol/L/min, $p<0.05$), but not maximal (0.46 ± 0.117 mmol/L/min at 0% buffer oxygen saturation), indicating residual oxidative metabolic capacity. HIF1α was also elevated, but not maximal. At this key threshold, ^{64}CuCTS deposited significantly more ^{64}Cu in the heart than any other tracer we examined, and more than twice that of ^{64}CuATSM (61.8 ± 9.6% injected dose versus 29.4 ± 9.5% $p<0.05$).
Conclusion: At the key hypoxia threshold required for maintained cardiac energetics, representative of survivable low grade cardiac ischaemia, only ^{64}CuCTS delivered a hypoxic:normoxic contrast of 3:1, a prerequisite for successful PET imaging. We are now translating this approach to *in vivo* tracer evaluation with a view to progressing successful candidates such as ^{64}CuCTS to clinical trial for imaging chronic cardiac ischemic syndromes.

The authors acknowledge financial support from the KCL BHF Centre of Research Excellence, BHF award RE/08/003 (project grant PG/10/20/28211) and a BHF Interdisciplinary Ph.D. studentship, the Department of Health via the National Institute for Health Research (NIHR) comprehensive Biomedical Research Centre award to Guy's & St Thomas' NHS Foundation Trust in partnership with King's College London and King's College Hospital NHS Foundation Trust, and the KCL and UCL Comprehensive Cancer Imaging Centre. Funded by the CRUK and EPSRC in association with the MRC and DoH (England). The views expressed are those of the authors and not necessarily those of the NHS, the NIHR or the Department of Health.

Where applicable, the authors confirm that the experiments described here conform with the Physiological Society ethical requirements.

C09

Longitudinal *in vivo* evaluation of colorectal tumour response to liposomal butyrate therapy using bioluminescence imaging

A. GOMEZ RAMIREZ[1], R. Bofinger[2], M. Ali[1], M. Zaw Thin[1], J. Connell[1], H. Hailes[2], A. Tabor[2], M.F. Lythgoe[1], T. Kalber[1] and J. Bell[3]

[1]Centre for Advanced Biomedical Imaging, UCL, LONDON, UK, [2]Chemistry, UCL, London, UK and [3]Life Sciences, University of Westminster, London, UK

Introduction - Butyrate is a short-chain fatty acid produced from microbial fermentation of dietary fibre in the human large intestine that inhibits proliferation, induces apoptosis and downregulates metabolic activity in colorectal cancer cells, while aiding healthy colonocyte function (1).
Oral and peripheral administrations of butyrate are limited by its short half-life (5min), ubiquitous nature, first-pass hepatic clearance and toxic dose. The objective of the present study is to evaluate the therapeutic potential of liposome-encapsulated butyrate for the treatment of colorectal cancer using bioluminescence imaging (BLI), tumour volume changes and ex vivo histological analysis.
Methods - Liposomes were formulated using a defined ratio of selected lipids (patent CA2882705A1)(2). Lipids dissolved in chloroform were dried *in vacuo* at 30°C using a rotary evaporator (Bucchi, UK) and hydrated using sodium butyrate (1M). Liposomes (100-150nm) were formed through ultrasonication (Fisher Scientific, UK) and sized using dynamic light scattering (DLS) (Malvern, UK). Non-encapsulated drug was removed by dialysis against a saline buffer solution (1M NaCl). Encapsulation efficiency was calculated using nuclear magnetic resonance (NMR) (400MHz; Bruker, UK).
Human LS174T colorectal adenocarcinoma cells were transfected with the firefly luciferase gene (LS174T_Luc+). Mice bearing LS174T-Luc+ subcutaneous tumours were chronically treated (3 times/week) with liposomes encapsulating butyrate or water (control) for 3 weeks (n=14). Tumour growth was tracked using BLI (luciferin

15mg/ml) and calliper-derived volumes. After therapy, mice were perfusion-fixed and tissues of interest were histologically analysed.
Results - The BLI data showed a significant decrease in BLI signal in butyrate treated tumours compared to controls within the first 10 days of treatment (Fig. 1; $p<0.05$). There were no significant differences in tumour volumes between groups, suggesting that metabolic downregulation in tumours does not directly correlate to tumour size.
Conclusions - This study is the first to evaluate the effect of liposomal butyrate on colorectal cancer *in vivo* using BLI. Since the production of photons from the catalysis of luciferin is dependent on adenosine triphosphate (ATP), the BLI data indicates that butyrate compromises the production of cellular energy thereby inducing metabolic downregulation in colorectal tumours. The fact that simultaneously tumour size was not significantly altered demonstrates the importance of evaluating therapeutic outcomes *in vivo* through non-invasive imaging methods. The present data promotes further evaluation of liposomal butyrate therapy, while its lack of toxicity highlights its potential as a preventive, pre-diagnostic and adjuvant treatment of colorectal cancer.

Figure 1. BLI measurement of subcutaneous LS174T+Luc tumour growth (%) after treatment with liposomes encapsulating butyrate or water (control) (±SD; n=14)

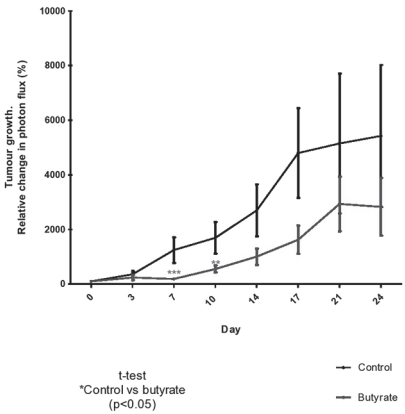

Figure 2. BLI time course images of a LS174T-Luc+ tumour-bearing mouse treated with **a)** control (water) liposomes and **b)** butyrate liposomes.

a)

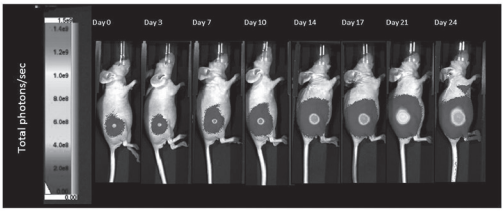

b)

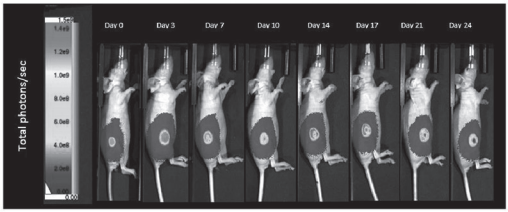

References

P. Louis et al (2014). The gut microbiota, bacterial metabolites and colorectal cancer. Nature Reviews Microbiology 12, 661–672.

J.D. Bell et al (2014). Nanoparticle formulation patent CA2882705A1 (2014) MRC, Imperial Innovations Ltd.

Acknowledgements

Dr T.Kalber's EPSRC Early Career Fellowship

CONACYT

Where applicable, the authors confirm that the experiments described here conform with the Physiological Society ethical requirements.

C10

Evaluation of the ligand [^{18}F]IMA201 as a novel radiotracer for aggregated alpha-synuclein in Parkinson's disease

E.J. Smyth[1], S. Tang[1], I. Ahmed[2], L.A. Wells[1], C. Plisson[1] and J. Passchier[1]

[1]Imanova Ltd, Hammersmith Hospital, London, UK and [2]Parkinson's UK Brain Bank, Centre for Neuroscience, Imperial College London, London, UK

Aggregated alpha-synuclein is one of the primary components of Lewy bodies which are a hallmark feature in the brains of patients with neurodegenerative diseases such as Parkinson's disease (PD). Currently, there are no imaging tools available to monitor α-synuclein in PD patients; a selective PET ligand would greatly help drug development efforts for PD in addition to the diagnosis and prognosis of α-synuclein associated diseases. The aim of this study was to evaluate [^{18}F]IMA201 as a potential PET ligand for delineation of α-synuclein in patients with PD.
Animal experiments were conducted in accordance with the UK Animals (Scientific Procedures) Act 1986 and human tissue was ethically sourced from the Parkinson's UK Brain Bank. [^{18}F]IMA201 was prepared following the recently developed copper II-mediated ^{18}F-fluorination methodology.[1] Anatomically adjacent fresh frozen tissue sections (10 μm) from the cortical region of three individual PD patients were cut and fixed in 4% paraformaldehyde. Sections were incubated with increasing concentrations of [^{18}F]IMA201 (0.3, 1, 10 nM) for 45 minutes, washed twice and apposed to phosphor-imager plates. Specific binding (SB) was identified by homologous block (10 μM) and ligand binding was quantified using a standard curve. The presence of α-synuclein was confirmed with immunohistochemistry in anatomically adjacent slides. Dynamic PET scans were conducted under baseline conditions (2.5 % isoflurane) and following pre-treatment with unlabelled IMA201 (2 mg/kg *i.v.*) to determine *in vivo* regional brain uptake of [^{18}F]IMA201 in a healthy male Sprague Dawley rat (n=1).
IMA201 was successfully labelled with ^{18}F with a radiochemical yield of 150-400MBq and mean specific activity of 10±11 GBq/μmol (n=3). [^{18}F]IMA201 demonstrated a heterogenous SB signal in brain tissue of three patients at three different concentrations (**0.3nM:** 6.2, 22 and 6.5 DLU/mm^2/Bq; **1nM:** 0, 120 and 40 DLU/mm^2/Bq; **10nM:** 390, 370 and 100 DLU/mm^2/Bq). Percentage SB ranged from 0 - 87%, which was consistent with the heterogenous expression of α-synuclein between patients as determined by immunohistochemistry. [^{18}F]IMA201 demonstrated good brain penetration in a healthy male rat with reversible kinetics during the time of the scanning period.
The successful labelling, SB characteristics and *in vivo* kinetic profile of [^{18}F]IMA201 suggest that this is a potential candidate for monitoring α-synuclein in the CNS. Radiosynthesis optimisation to allow clinical translation and further studies investigating the selectivity of [^{18}F]IMA201 for α-synuclein over other misfolded proteins in patient brains, including the evaluation of a SB signal in a rodent model of PD,

are required to confirm the potential of [^{18}F]IMA201 in clinical applications and neurodegenerative drug development.

C. Plisson *et al. (2015). J Label Compd Radiopharm*, **58** (S1), S268.

Where applicable, the authors confirm that the experiments described here conform with the Physiological Society ethical requirements.

C11

Magnetic Resonance Imaging (MRI) reveals multiple facets of gastric motor function in Ehlers-Danlos Syndrome (hypermobility-type) (EDS-HT): A Preliminary Study

Heather Fitzke, UCL / QMUL, UK

BACKGROUND: Functional dyspepsia (FD) characterised by unexplained symptoms of early satiety, bloating and abdominal pain[1] substantially burden patients and healthcare systems. Recent observations suggest 50% of FD patients meet the criteria for Ehlers-Danlos Syndrome Hypermobility Type(EDS-HT)[2-4]. Novel magnetic resonance imaging (MRI) techniques [5-10] allow measurement of gastric motor function in EDS-HT patients to investigate symptoms of dyspepsia – non-invasively in a single exam[11, 12].

METHODS: 6 female EDS-HT patients (mean age 34, range 26 - 50) with FD were recruited via tertiary referral and matched by age, sex and body-mass index(BMI) to healthy controls (n=6). Informed consent was obtained for an MRI scan following >4hrs fast, with EDS-HT patients suspending use of motility affecting medications ~4days before. Anatomical (20s breath hold, balanced steady state, coronal, 5mm TR =3.3ms, TE =1.58ms) and motility (free breathing, BTFE, coronal, temporal resolution=0.3s, 10mm slice, TR=2.97ms, TE=1.49ms) data were acquired in the prone position on a Philips Achieva 3T MRI. Subjects consumed 300ml water and scans repeated every 10min-1hr. 2 readers manually segmented the stomach images and inter-reader agreement assessed (Pearson's correlation coefficient). Data were analysed using paired t-test for: A) Gastric emptying (time for 50% of the water to clear stomach, adjusted for baseline); B) Gastric accommodation (% change in volume following water challenge) & C) Gastric motility (contractions per minute, cpm) (Fig 1)

RESULTS: The protocol was tolerated well and inter-reader agreement was 0.97.
A) Gastric emptying: EDS-HT mean time was 16 min (range 8 to 26) vs. 25 min (range 8 to 30) for controls, p = 0.04.
B) Gastric accommodation: EDS-HT showed an increase in volume of 244% (range 82 to 468%) and in controls 317% (range 170 to 567%) with a mean difference of 73%, n.s
C) Gastric motility (contractions per min, cpm): EDS-HT mean 1.1cpm (range 0 to 2.7) was significantly lower than controls 2.9cpm (range 2.3 to 3.6), p = 0.006.

CONCLUSIONS: MRI is a well-tolerated method with high inter-reader agreement for quantitatively assessing gastric function, without additional contrast. The accelerated gastric emptying of liquid in EDS-HT patients suggests that symptoms of early satiety may be of duodenal origin. That this occurs alongside reduced motility, suggests that disturbances in gastric motor activity and the origin of

symptoms are multi-dimensional and may delay solid emptying more than liquid emptying. Further investigation of gastric function using MRI, in a larger series of patients, using both liquids and solids is required to provide further insight to the pathophysiology of dyspeptic symptoms in patients with EDS-HT.

REFERENCES

1. Zarate, N., et al., Unexplained gastrointestinal symptoms and joint hypermobility: is connective tissue the missing link? Neurogastroenterology & Motility, 2010. 22(3): p. 252-e78.
2. Eckberg. 1976. J Physiol. Temporal response patterns of the human sinus node to breif carotid baroreceptor stimuli.pdf>.
3. Castori, M., et al., Management of pain and fatigue in the joint hypermobility syndrome (a.k.a. Ehlers–Danlos syndrome, hypermobility type): Principles and proposal for a multidisciplinary approach. American Journal of Medical Genetics Part A, 2012. 158A(8): p. 2055-2070.
4. Castori, M., et al., Connective tissue, Ehlers–Danlos syndrome(s), and head and cervical pain. American Journal of Medical Genetics Part C: Seminars in Medical Genetics, 2015. 169(1): p. 84-96.
5. Akerman, A., et al., Computational postprocessing quantification of small bowel motility using magnetic resonance images in clinical practice: An initial experience. J Magn Reson Imaging, 2016.
6. Hoad, C.L., et al., Colon wall motility: comparison of novel quantitative semi-automatic measurements using cine MRI. Neurogastroenterol Motil, 2015.
7. Menys, A., et al., Comparative quantitative assessment of global small bowel motility using magnetic resonance imaging in chronic intestinal pseudo-obstruction and healthy controls. Neurogastroenterol Motil, 2016. 28(3): p. 376-83.
8. Menys, A., et al., Dual registration of abdominal motion for motility assessment in free-breathing data sets acquired using dynamic MRI. Phys Med Biol, 2014. 59(16): p. 4603-19.
9. Menys, A., et al., Global small bowel motility: assessment with dynamic MR imaging. Radiology, 2013. 269(2): p. 443-50.
10. Odille, F., et al., Quantitative assessment of small bowel motility by nonrigid registration of dynamic MR images. Magn Reson Med, 2012. 68(3): p. 783-93.
11. Fikree, A., et al., Functional gastrointestinal disorders are associated with the joint hypermobility syndrome in secondary care: a case-control study. Neurogastroenterol Motil, 2015. 27(4): p. 569-79.
12. Valcourt, U., et al., Tenascin-X: beyond the architectural function. Cell Adhesion & Migration, 2015. 9(1-2): p. 154-165.

Emptying

Total volume of stomach (excluding gas) measured pre & post challenge.

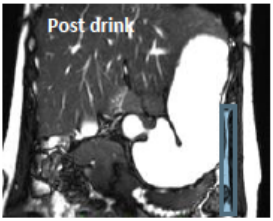

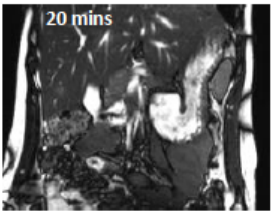

Volumetric measurements made a minimum of 4 times over an hour.

Accommodation

Total volume of stomach (including gas) measured above incisura pre & post challenge

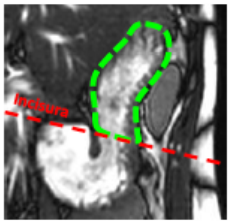

H_2O Challenge

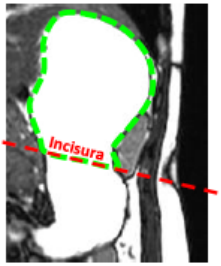

Motility

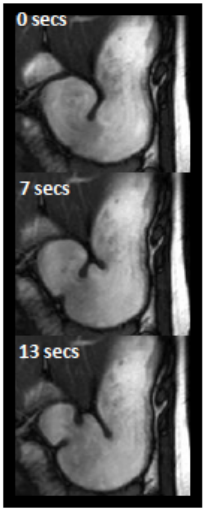

Contractions counted semi-quantitatively pre and post water challenge.

C12

Multi-modal multi-scale whole-body *in vivo* imaging to track spontaneous cancer metastasis and treatment response

Alessia Volpe, King's College London, UK

Imaging spontaneous cancer cell metastasis or responses to drug treatment in vivo is difficult to achieve. Here the goal was to develop a highly sensitive and reliable pre-clinical longitudinal in vivo imaging model for this purpose thereby facilitating mechanistic understanding of cancer metastasis as well as discovery and validation of anti-cancer therapies or molecular imaging agents. The strategy is based on cancer cells stably expressing the human sodium iodide symporter (NIS) fused to a fluorescent protein, thereby permitting radionuclide and fluorescence imaging[1]. Using whole-body nanoSPECT-CT with 99mTcO4- we followed primary tumour growth and spontaneous metastasis in various tumour models (breast, melanoma) and assessed the effects of the drug etoposide on metastasis. NIS imaging was used to classify organs as small as individual lymph nodes (LN) to be positive or negative for metastasis and results were confirmed ex vivo by confocal fluorescence microscopy. This metastasis tracking strategy was applied to various cancer models including xenograft models of spontaneous metastasis in breast cancer and melanoma.

In a breast adenocarcinoma model, we found our NIS-based metastasis tracking strategy to out-perform state-of-the-art [18F]FDG-afforded cell tracking in its ability to detect small tumours (18.5-fold better tumour:blood ratio) and metastases (LN: 3.6-fold) due to improved contrast in organs close to metastatic sites (12- and 8.5-fold lower SUV in heart and kidneys, respectively). We further demonstrate that a chemokine receptor truncation results in enhanced metastasis, in particular lymph node metastasis, as compared to the full-length receptor. Furthermore, we applied the model to assess the treatment response to the neo-adjuvant etoposide and found a heterogeneous response to the treatment depending on the microenvironments (tumour vs. metastatic site), which was only detected with the NIS-based tracking strategy but not when using [18F]FDG. Importantly, in the 4599 melanoma model we were for the first time able to demonstrate spontaneous metastasis in vivo in a longitudinal imaging experiment. We found lung metastases established 21 days post tumour implantation in NOD/SCID/γ mine while other sites were not affected at that time point.

In conclusion, our NIS-fluorescent protein-based dual mode radionuclide-fluorescence imaging approach to in vivo track cancer cell metastasis proved a valuable tool for mechanistic as well as pharmacologic interventional studies.

[1] Fruhwirth GO, Diocou S, Blower PJ, Ng T and Mullen G.E.D. A Whole-Body Dual-Modality Radionuclide Optical Strategy for Preclinical Imaging of Metastasis and Heterogeneous Treatment Response in Different Microenvironments. 2014. Journal of Nuclear Medicine;55(4):686-94.

C13

Visualisation of Caspase Activity using Fluorescence Lifetime Optical Projection Tomography in Live Zebrafish

Natalie Andrews, Imperial College London, UK

Current microscopy techniques are not optimal to image fluorescence in whole live animals. We present fluorescence lifetime optical projection tomography (FLIM OPT) applied to imaging enzyme activity in live transgenic zebrafish expressing FRET biosensors.

OPT can be considered the optical equivalent to x-ray CT. Samples are rotated through 360 with images acquired at set intervals, and a back projection technique is applied to reconstruct the 3D image1. It can be performed in transmission or fluorescence modes, allowing a wide range of visualisation techniques, including FLIM. Combination of OPT with FLIM provides a means to study enzyme activity in 3D through Förster Resonance Energy Transfer (FRET). The optimal size range for OPT is mm-cm, filling a size gap between confocal and MRI, which is also the size range for zebrafish, making them an ideal model for imaging. There are also transparent mutant lines available, such as the TraNac. These were used to generate transgenic zebrafish expressing FRET biosensors for Caspases 1 and 3 ubiquitously. For all experiments, fish were mounted in agarose containing 4.2% MS222. For OPT they were mounted in FEP tubing, for confocal on a cover slip. During OPT images were acquired every 4° using 5 time gates and for confocal TCSPC was used. All FLIM data was fitted using FLIMfit2. Caspase 3 is an apoptotic enzyme thus to induce apoptosis, 1 day post fertilisation (dpf) Tg(Ubi:Caspase3bios) embryos were irradiated with 25 Gy gamma irradiation from a 137Cs source after which fish were imaged cross sectionally3. At 3.5 hours post irradiation an increase in fluorescence lifetime was visible in the head region (Figure 1A, B) indicative of biosensor cleavage and Caspase 3 activity. Through development of 3D ROI quantification techniques we were able to show this was a statistically significant increase ($p<0.01$, Figure 1C). Following the validation of FLIM OPT to monitor enzyme activity, we have begun to validate a novel Caspase 1 FRET biosensor. Caspase 1 is activated as part of the inflammasome, and a standard assay to study inflammasome activation in zebrafish is tail transection (TT). 4 dpf Tg(Ubi:Caspase1bios) embryos underwent TT and were imaged via confocal FLIM. An increase in lifetime was seen at the sight of wounding, indicative of a functional biosensor and Caspase 1 activity.

In conclusion, FLIM OPT is an effective method to detect enzyme activation in 3D over a whole organism. We have developed a functional Caspase 3 FRET biosensor and have preliminary data suggesting a novel, functional Caspase 1 FRET biosensor. Figure 1 25Gy induces apoptosis in the head region of 1 dpf Tg(Ubi:Caspase3bios) zebrafish embryos. A) 1 hpi B) 3.5 hpi C) number of pixels with a lifetime over 2 ns

per fish. Statistical analysis was carried out using one way ANOVA with Bonferronis post test. N> 8.

1. Sharpe, J., Ahlgren, U., Perry, P., Hill, B., Ross, A., Hecksher-Sørensen, J., Davidson, D. (2002). Optical projection tomography as a tool for 3D microscopy and gene expression studies. Science (New York, N.Y.), 296(5567), 541–5.
2. Warren, S. C., Margineanu, A., Alibhai, D., Kelly, D. J., Talbot, C., Alexandrov, Y., French, P. M. W. (2013). Rapid global fitting of large fluorescence lifetime imaging microscopy datasets. PloS One, 8(8), e70687.
3. Andrews, N., Ramel, M.-C., Kumar, S., Alexandrov, Y., Kelly, D. J., Warren, S. C., Kerry, L., Lockwood, N., Frolov, A., Frankel, P., Bugeon, L., McGinty, J., Dallman, M. J. and French, P. M. W. (2016), Visualising apoptosis in live zebrafish using fluorescence lifetime imaging with optical projection tomography to map FRET biosensor activity in space and time. J. Biophoton., 9: 414–424.

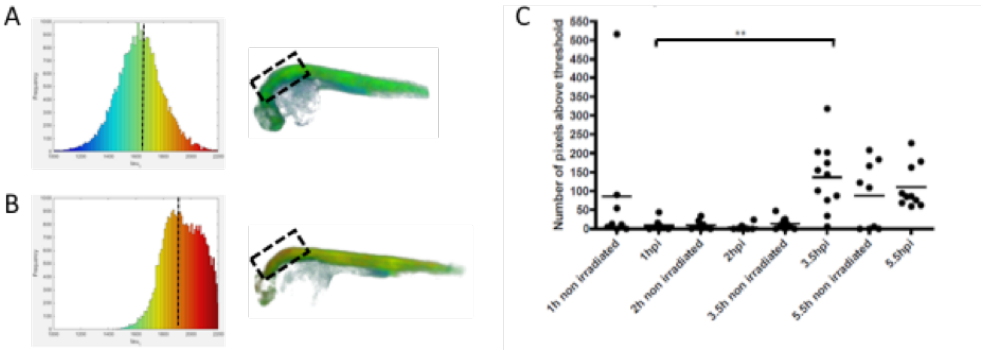

C14

Monitoring liver fibrosis disease progression and resolution with cell therapy

John Connell, University College London, UK

Introduction

Liver fibrosis is a significant health problem with worldwide mortality. Regenerative stem cell therapies could play a major role in the control of this disease. There is therefore a need for translatable longitudinal non-invasive imaging read outs of fibrosis that can assess success of regenerative cell therapies. The whole body biodistribution and local organ retention of cell therapies must also be observed in the early preclinical stage to help predict outcome and cell fate. Liver disease in humans can be quantitatively assessed in patients using T1 and T2* mapping (1). The work presented here aims to characterise a mouse model of liver fibrosis using quantitative MRI parameters as well as monitoring the biodistribution and fate of implanted cell therapy to assess whether MRI can detect fibrosis resolution after cell therapy.

Methods

Quantitative T1 and perfusion maps of the mouse liver were acquired with an inversion recovery, spoiled Look-Locker gradient echo sequence with retrospective gating (2) under anaesthesia with 100% O2 or medical with 10% CO2 as the carrier gas. A respiratory-triggered, gradient echo sequence was used for T2*maps. Mice received up to 3 months of carbon tetrachloride injections (n=12) or controls (n=5). Bone marrow was extracted from the femurs and tibias of a mouse and incubated with macrophage colony stimulating factor and engineered to express luciferase. 300,000 bone marrow derived macrophages (BMDMφ) were injected into the hepatic portal vein via guidance by ultrasound and in vivo cell tracking was performed with bioluminescence imaging. Liver fibrosis was confirmed using histology of picosirius red.

Results

The mean T1 value across the liver was significantly increased (1408±13.5 ms vs. 1473±10.7 ms) and the mean T2* showed a non-significant decrease (10.18±0.70 ms vs. 9.21±0.30 ms) in mice bearing liver fibrosis compared to age-matched controls. Additionally, the increase in blood perfusion in the liver during CO2 gas challenge was significantly reduced in mice bearing liver fibrosis (3.81±0.42 vs 2.80±0.24 ml/min/g). Injected BMDMφ were detected in the liver and peritoneum up to 10 days after implantation.

Discussion

The results presented here show that quantitative MRI parameters can be used to monitor the onset of experimental liver fibrosis in a similar fashion to clinical findings (1). A novel functional response of the liver was developed in response

to hypercapnea which can identify disease pathology at an early stage. This can be used to monitor disease status as a platform for measuring the efficacy of novel cell therapies. Bioluminescent imaging has been utilised to successfully track bone marrow derived macrophages at the organ of interest and has shown that they are viable for at least ten days. Studies are ongoing to assess whether these MRI parameters can evaluate therapeutic change in liver fibrosis after cell therapy.

(1) Banerjee et al., J Hepatol (2014)
(2) Ramasawmy et al., NMR Biomed (2015)

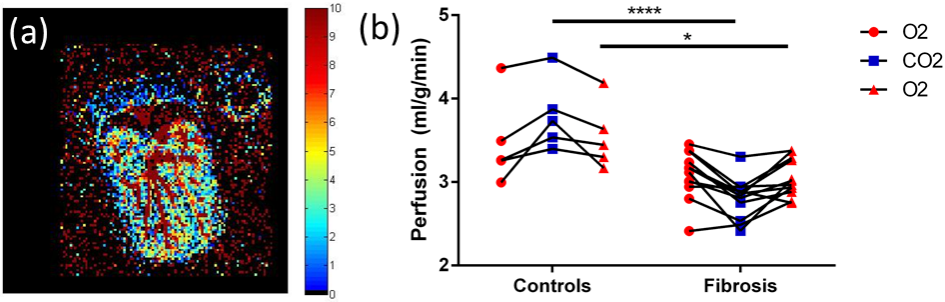

Figure 1
Typical perfusion map (ml/min/g) of axial plane of mouse abdomen (a). A region of interest was drawn across the parenchyma and applied to three sets of perfusion map data under a hypercapnia gas challenge. (b) control mice showed a higher increase in perfusion while breathing 10% CO2 compared to mice with liver fibrosis (2-way ANOVA with Sidak's test)

C15

X-ray excitation of CdTe quantum dots

Sean Ryan, University of Hertfordshire, UK

We report positive detections of near-infrared (NIR) emission from aqueous suspensions of CdTe quantum dots excited by X-rays at keV energies. Using a clinical X-ray source, detectable emission was obtained with 1 second duration X-ray exposures and 1 second duration optical integration times, suggesting that the development of pre-clinical imaging modalities using quantum dots as NIR beacons will be feasible with readily obtainable X-ray fluences and practical (suitably short) measurement times.

Ryan, S. G., Butler, M. G., Adeyemi, S. S. & Lythgoe, M. 2016, in prep.

C16

Novel multi-modal imaging agent for stem cell tracking

May Zaw Thin, University College London, UK

Introduction

Stem cell therapy potentially provides treatment for a variety of diseases. However, tracking cell distribution throughout the body is challenging. Labelling with Indium-111 (111In)-oxine for Single Photon Emission Computed Tomography (SPECT) is disadvantageous as it causes cytotoxicity and leakage of the tracer. The aim of this study was twofold; 1) to reduce cytotoxicity of radiolabeling1, and 2) conjugate 111In to superparamagnetic iron oxide nanoparticles (SPION)2 via a 1,4,7,10-tetraazacyclododecane-1,4,7,10-tetraacetic acid (DOTA) for multi-modality imaging with both SPECT3 and magnetic resonance imaging (MRI).

Methods

DOTA was functionalized with an amine group which was used to form a peptide bond with carboxyl groups on FluidMAG-CT(Chemicell). 111In was chelated using HEPES buffer (pH 5.5) with magnetic purification. Luciferase positive human adipocyte derived stem cells (ADSC) were incubated with 111In-SPION at 37°C overnight (Figure 1a). 1.5 x 105 cells (containing 1.3 MBq of 111In, 140µg of Fe) were injected intravenously or ultrasound guided left ventricular intracardiac injection into NOD/SCID mice. Mice were imaged with bioluminescence (BLI – AMI-X SI Imaging), SPECT-CT (NanoscanSPECT-CT Mediso) and MRI (9.4T Agilient) and at 1, 24, 72 h and 7 days after injection. SPECT images were obtained using 1 mm pinhole apertures with 90s per view. MR images were acquired using a fast spin echo multi-slice sequence (T2 and T2*-weighted images).

Results

1h after intravenous injection, SPECT/CT images showed dual labelled ADSCs were in lungs (50%) and liver (10%). This correlated with BLI showing signal from lungs and with MRI which showed a reduction in T2 in the liver (Figure 1b,c,d). By comparison, SPECT/CT images at 1h after intracardiac injection showed ADSC distribution was predominantly in liver (42%) and certain percentage in lungs, kidney

and brain. This correlated with BLI and with MRI which showed focal black spots in the brain indicating the presence of dual labelled cells (Figure1e,f,g). BLI showed cells remained viable for 20 days after both injection routes. Low SPECT signal in the bladder suggested no leakage of 111In.

Conclusions

These results demonstrate the advantages of combining a genetic BLI reporter with a novel SPECT/MRI nanoparticle to quantitatively assess whole body distribution of ADSC after different injection routes. DOTA chelation of 111In also effectively stops dissociation of the tracer and limits cytoxicity. This novel multimodal imaging strategy can be applied to a range of models, allowing valuation of successful delivery to target organs and cell survival.

1) McLean et al. 1989 Biochem Cell Biol, 2) Torres et al. 2011 Bioconjug Chem 3) Mitchell et al. 2013 Biometarials.

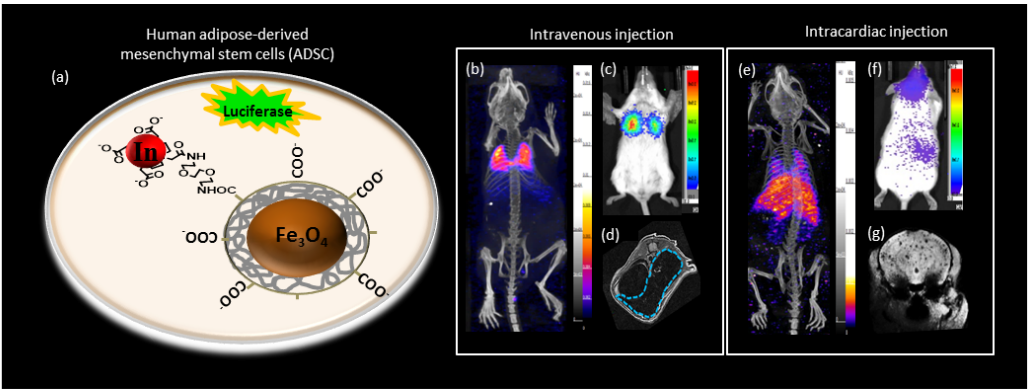

Figure1:(a)Schematic diagram of ADSC containing DOTA chelated ^{111}In-SPION with luciferase(b, c, d)ADSC distribution at 1h after intravenous injection showing SPECT/CT image of radiolabelled cells in lung and liver, BLI image of viable cells in lung and T2–weighted MR image of SPION labelled cells in liver(e, f, g) ADSC distribution at 1h after intracardiac injection showing SPECT/CT image of radiolabelled cells in liver, BLI image of viable cells in brain and liver and T_2*-weighted MR image of SPION labelled cells in brain.

C17

Multimodal *In Vivo* Imaging of CAR T Cell Therapies of Brain Malignancies

Tammy Kalber, University College London, UK

Introduction: Chimeric antigen receptor (CAR) T-cell therapy is emerging as an effective strategy in neuro oncology. The therapy has already had some remarkable results in haematological cancers with some patients showing complete remission. However, the response is varied and the treatment of solid malignancies has so far been limited. Non-invasive imaging using genetic reporters plays a key role in determining the fate of therapeutic genes and cells but neuro imaging is challenging due to the blood brain barrier (BBB). In this study we utilize the firefly luciferase gene reporter (Fluc) to assess the ability of CAR T cells to target solid brain tumours in a mouse glioma model and measure the resulting therapeutic effect by magnetic resonance imaging (MRI). Secondly, we propose a novel nuclear genetic reporter based on the human dopamine transporter (hDAT) and the FDA approve radiotracer [123I]-FP-CIT (DatSCAN). DatSCAN is used to assess Parkinson's disease and has been shown to cross the BBB.

Methods: Bioluminescent (BLI) therapy model: C57b/6 mice were given a stereotactic injection of 2 x106 GL261 murine glioblastoma cells (EGFRv111 +ve) cells into the striatum. At day 11 mice were image using a 1T Bruker Icon MRI system using a T2-weighted sequence (TR = 3201.5 ms, TE = 85 ms, flip angle = 90°, 20 □ 20 mm2 field of view, 96 □ 96 matrix, slice thickness = 0.5 mm, 30 averages). The day after mice received either 5x106 EGFRvIII CAR Fluc transduced T cells or the same number of CD19 CAR Fluc (control) T cells. Mice were imaged with BLI (PhotonOptima, Biospace) and MRI at days 15, 18 and 24 post glioma injection. Novel hDAT model: Human SupT1 cells were engineered to express hDAT and FLuc. Tracer binding was validated by incubating hDAT(+) and hDAT(−) cells with DatSCAN. Specificity was determined by co-incubation with cold compound ([I]-FP-CIT). 10x104 hDAT Fluc double transduced SupT1 cells were injected into the striatum of NSG mice. Cell viability and proliferation was verified by BLI and tumour size by T2 MRI. DatSCAN uptake within the brain was characterised by Single Positron Emission Computer Tomography (SPECT) and overlaid on Computer Tomography (CT) images at 0.15, 2, 4, and 6 h post i.v. injection. The SPECT data was co-registering to the MRI data.

Results: Bioluminescent (BLI) therapy model: MRI showed that the GL261 tumour growth was fairly uniform in size at day 11. EGFRvIII CAR Fluc T cells showed a significantly higher uptake by BLI (107 p/s/sr) than control CD19 CAR Fluc T cells (105 p/s/sr), and expanded over the time course of the study (Fig 1a). There was also a reduction in tumour size by MRI in the EGFRvIII CAR Fluc T cell treated tumours compared to that of CD19 controls but this was not significant (Fig 1b). This suggests that CAR T cells can cross the BBB and effective in treating solid brain

tumours.
Novel hDAT model: hDAT (+) SupT1 cells demonstrated a significantly higher uptake of DatSCAN (25.08% □ 1.14) compared to hDAT(-) cells (0.31% □ 0.04). Co-incubation with cold [I]-FP-CIT significantly reduced this (1.01 ± 0.22). BLI confirmed in vivo hDAT(+) SupT1 viability and expansion (Fig 1c). The in vivo binding potential of DatSCAN was monitored by SPECT/CT and peaked at 2h, decreasing at 4h, and 6h (Fig 1d). The SPECT images show uptake in the tumour but also the basil ganglia, images at 2h were co-registered to tumour MRI (Fig 1d).

Conclusion: This study demonstrates for the first time that CAR T-cells can be visualised in the brain, and that they show migration and expansion in an antigen dependent manner. The reduction of tumour size by MRI of GL261 tumours treated with EGFRVIII Fluc T cells also showed that CAR T cells are therapeutic to solid brain malignancies but may not be sufficient to completely eradicate tumours. The use of the hDAT reporter system with DatSCAN provides a clinically translatable means of monitoring real time confirmation of CAR T cell uptake and therapeutic response. However, further characterization is needed to assess if hDAT is suitable to monitor CAR T cell migration to diffuse brain tumours.
Fig 1: A) MRI of GL261 tumours pre-treatment at day 11, and BLI of subsequent CAR T cell uptake (EGFRvIII or Control CD19) at days 15, 18, and 24. B) MRI of GL261 tumour size pre-treated (top row) and post treated (EGFRvIII or Control CD19), and a graph of tumour volumes. C) BLI indicating hDAT (+) SupT1 cells in the brain, and uptake of DatSCAN by SPECT/CT over 6 hours showing signal the tumour and background basal ganglia. D) SPECT/CT co-registration with MRI data (B = basal ganglia, T = tumour).

T.L. Kalber [1], G. Agliardi[1,2], L. Kiru[1,3], B. Philip3, A. Badar[1], A. Jathoul [3], K. Straathof[3], J.C. Anderson [2], M. Pule[3], M.F. Lythgoe[1]

[1] Centre for Advanced Biomedical Imaging (CABI), Division of Medicine, University College London, 72 Huntley Street, London, WC1E 6DD UK.
[2] UCL Institute of Child Health, University College London, 30 Guilford Street, London, WC1N 1EH UK.
[3] UCL Cancer Institute, University College London, 72 Huntley Street, London, WC1E 6DD UK.

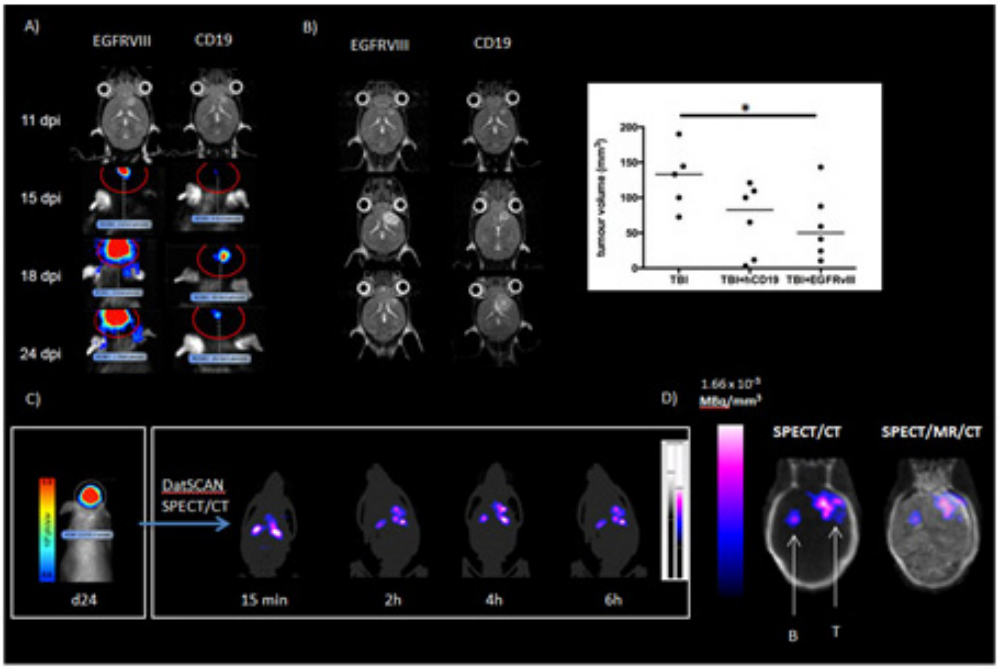
A)
EGFRVIII
CD19
11 dpi
15 dpi
18 dpi
24 dpi
B)
EGFRVIII
CD19
tumour volume (mm³)
200
150
100
50
0
TBI
TBI+hCD19
TBI+EGFRvIII
C)
d24
DatSCAN
SPECT/CT
15 min
2h
4h
6h
D)
1.66 x 10⁻⁵
MBq/mm³
SPECT/CT
SPECT/MR/CT
B
T

C18

PET imaging of tumor glycolysis downstream of hexokinase through noninvasive measurement of pyruvate kinase M2

Tim Witney, Stanford University, USA

Cancer cells reprogram their metabolism in order to meet increased biosynthetic demands, commensurate with elevated rates of replication [1]. Aberrant tumor glycolysis has long been known to support the synthesis of metabolic precursors required to sustain this anabolic phenotype [2]. Pyruvate kinase catalyzes the final and rate-limiting step in glycolysis, with the M2 spliced isoform (PKM2) purported as a key regulator of aerobic glycolysis in tumors [3]. We report here the synthesis and evaluation of a novel positron emission tomography (PET) radiotracer, [11C] DASA-23, that provides a direct measure of PKM2 expression for ther first time, using preclinical models of glioblastoma multiforme (GBM). PKM2-23 was labeled with 11C (t1/2 = 20.4 min) at its aromatic methoxy moiety from the corresponding nor-derivative of DASA-23 and the highly efficient methylation reagent [11C] CH3OTf, with a radiochemical yield of 2.3 ± 0.8%, >99% radiochemical purity and a specific activity of 5.4 ± 2.8 Ci/μmol at end of synthesis (EOS; n = 7). [11C] DASA-23 cell uptake strongly correlated with PKM2 protein expression in cultured tumor cells (R2 = 0.83; P = 0.005; n = 3), assessed through target modulation by short inhibitory RNA (sense, CCAUAAUCGUCCUCACCAAUU; antisense, UUGGUGAGGACGAUUAUGGUU). In vivo, orthotopic U87 and patient-derived GBM39 tumors were clearly delineated from the surrounding normal brain tissue by dynamic PET imaging (n = 6 mice; Fig. 1). By 30 min post injection, [11C] DASA-23 radioactivity in U87 tumors was 1.68 ± 0.47 %ID/g versus 0.78 ± 0.18 %ID/g in the contralateral background tissue (n = 6; P = 0.003). PET/MR co-registration confirmed precise correspondence of the [11C]DASA-23 signal with the location of the intracranial tumors, further confirmed ex vivo by autoradiography, histopathology, and exclusive tumor-associated PKM2 expression. PKM1 expression was confined to the healthy brain and was not present in the tumor. In longitudinal studies, systemic treatment of orthotopic GBM39-tumored mice with the PKM2 agonist, TEPP-46, resulted in a reduction of tumor-associated [11C]DASA-23 to background levels, from 1.61 ± 0.12 %ID/g to 0.88 ± 0.13 %ID/g (45% decrease; n = 4; P = 0.0002). Together, these data demonstrate that [11C]DASA-23 annotates tumor-associated PKM2 in preclinical models of human GBM and provides the basis for clinical evaluation of imaging agents that target this important gatekeeper of tumor glycolysis. Given the great interest in targeting PKM2 for cancer therapy [4], [11C]DASA-23 may also provide a means to measure the therapeutic efficacy of these novel agents.

Fig 1. Non-invasive imaging of mice bearing orthotopic U87 human gliomas. (a) Chemical structure of [11C]DASA-23. (b) Representative fused [11C]DASA-23-PET/CT (10 – 30 min summed activity) 3D volume rendering technique (VRT) image of the head of a mouse containing an orthotopically-grown U87 tumor. Grey scale is CT image and colour scale is PET image. The long white arrow indicates the tumor. [11C]DASA-23 accumulation in the harderian glands is indicated by white arrow heads. (c) Orthotopic U87 tumor and corresponding contralateral normal brain TAC taken from dynamic [11C]DASA-23-PET/CT images. Data is mean ± SD (n = 6 animals). (d) Representative contrast-enhanced T1-weighted MR coronal and horizontal images of orthotopically-implanted U87 gliomas. (e) Corresponding merged [11C]DASA-23-PET/MR images (10 – 30 min summed [11C]DASA-23 activity). Arrows and dashed circles indicate regions of contrast enhancement and radiotracer uptake, thought to correspond to tumor tissue. (f) Histopathological and ex vivo autoradiography analysis of orthotopic U87 human GBM. Arrows indicate the tumor. ***, $P < 0.01$.

[1] Cairns RA, Harris IS and Mak TW (2011) Regulation of cancer cell metabolism. Nat Rev Cancer 11: 85-95.
[2] Gatenby RA and Gillies RJ (2004) Why do cancers have high aerobic glycolysis? Nat Rev Cancer 4: 891-899.
[3] Wong N, De Melo J and Tang D (2013) PKM2, a Central Point of Regulation in Cancer Metabolism. Int J Cell Biol 2013: 242513.
[4] Anastasiou D, Yu Y, Israelsen WJ, Jiang JK, Boxer MB, et al. (2012) Pyruvate kinase M2 activators promote tetramer formation and suppress tumorigenesis. Nat Chem Biol 8: 839-847.

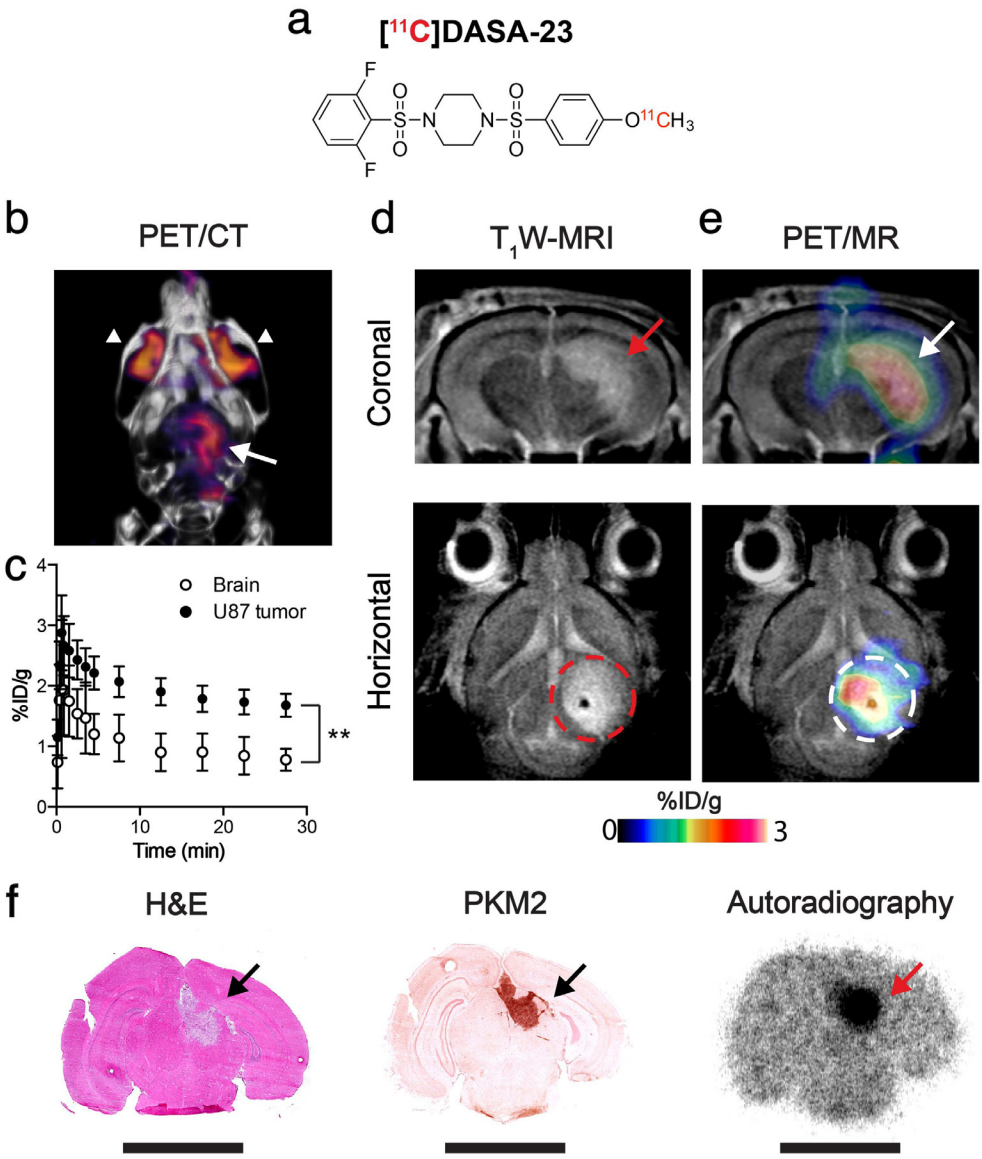
a
[11C]DASA-23
F
O
S
N
N
S
O
O11CH3
F
b
PET/CT
c
Brain
U87 tumor
%ID/g
4
3
2
1
0
0
10
20
30
Time (min)
**
d
T1W-MRI
e
PET/MR
Coronal
Horizontal
%ID/g
0
3
f
H&E
PKM2
Autoradiography

C19

MRI characterisation of iron overload in a humanised mouse model of β-thalassemia major

Laurence Jackson, University College London, UK

Introduction: β-thalassemia major is a common blood disorder causing the synthesis of abnormal haemoglobin leading to severe anaemia. Current disease treatment consists of regular blood transfusions a consequence of which is iron overload. MRI evaluation of iron loading is key to the clinical management of patients with thalassemia [1]. Research into therapy has been limited due to difficulties in producing a clinically relevant animal model of the disease. A novel humanised mouse model of thalassemia developed by Huo et al. [2] in which heterozygous animals are affected by anemia, splenomegaly and extramedullary hematopoiesis, provides a platform for the development of new treatments in a clinically relevant model. Here we show that MRI can be used to assess and quantify disease in vivo providing a method for serial long term assessment of the efficacy of therapies in rodents.

Methods: γHPFHδβ0/γβA knockin heterozygous thalassemia mice (n=6) received intraperitoneal injections of iron dextran solution (100mg/ml for 4 weeks (5days/week)) to simulate repeated blood transfusions. Two control groups 1) wild type humanised controls γβA/γβA, n=7 and 2) γHPFHδβ0/γβA knockin heterozygous thalassemia mice, n=6 received injections of PBS. MR imaging was performed at 5 months of age using a 9.4T (Agilent technologies, USA) system equipped with 1000mT/m gradients and a 39mm volume resonator RF coil (Rapid biomedical, Germany). Spleen volume was measured using a gradient echo (GE) structural scan (156×156×500μm). Cardiac function was measured using a standard cine GE sequence segmented at systole and diastole to quantify ejection fraction (EF). T1 was measured using an inversion recovery look locker (LL) sequence ($2.8 \leq TI \leq 30 \times RR$ interval (~110) [ms]) with regional means fitted to a LL corrected T1 relaxation curve. T2 was measured using a ECG+RESP gated spin-echo multislice sequence with 8 echo times ($2.7 \leq TE \leq 20$[ms]). T2* was measured with an ECG+RESP gated multi-GE sequence with 15 echo times ($0.9 \leq TE \leq 14.9$[ms]). T2 and T2* regional means were fitted to a standard T2 spin relaxation curve. Non-haem iron concentration was measured in excised heart, spleen and liver using the Bothwell iron assay.

Results: Spleen volume to animal mass ratio was significantly higher in control thalassemia (9.5±1.2mm3/g) and iron overload thalassaemia mice (9.1±1.3mm3/g) relative to wild type mice (4.0±0.4mm3/g). Representative T2w images in Figure 1 demonstrate the strong influence of high iron content on T2 relaxation in the liver (Lvr) and heart (Myo). Quantitative assessment showed that Iron overload reduced T1, T2 and T2* in all organs measured, while thalassemia reduced T2 in the liver and spleen, and T2* in the liver relative to wild type mice Table 1.

Table 1 – Relaxation times for tissues, * $p < 0.05$ relative to WT control, † signifies unquantifiable data. Given as mean±SEM

Quantification of non-haem tissue iron made using the Bothwell assay allows animal-specific correlations with relaxometry measurements, for example figure 2 shows evidence of correlation between liver iron with T2 relaxation.

Discussion: Hypersplenia observed in the thalassemia mice is a consequence of increased iron deposition in the organ due to poor processing of abnormal RBCs. This increased iron content shortened spleen and liver T2 and T2*, as confirmed by tissue iron assays. MR relaxation in the heart was unaffected by thalassemia, possibly due to the relatively early analysis time point, however T1, T2 and T2* were shortened in iron loaded animals making these measures useful for assessment of iron chelation therapies.

Conclusion: MR imaging techniques can identify thalassemia mice through increased spleen volume and shortened T2 and T2* in the spleen and liver. Iron overload shortened T1, T2 and T2* in the heart, liver and spleen. These imaging methods provide a platform for assessing the severity of thalassaemia by the accumulation of iron in these organs in-vivo allowing for serial assessment and development of preclinical therapies such as iron chelation and gene therapy.

[1] Huo et al, Annals New York AcademySciences 2010, 1202, 45. [2] Carpenter et al, Circulation 2011, 123, 1519-1528

	T1 [ms]			T2 [ms]			T2* [ms]		
	Wild type	Thalassaemia		Wild type	Thalassaemia		Wild type	Thalassemia	
	Control	Control	Overload	Control	Control	Overload	Control	Control	Overload
Heart	1157±51	1366±89	**470±68***	23.8±2.5	**15.3±2.1***	**3.3±0.3***	11.7±1.7	10.3±2.3	**0.8±0.1***
Liver	933±53	1014±127	**415±41***	14.2±0.9	**9.5±1.3***	**1.3±0.1***	9.2±0.6	**4.8±0.7***	**2.4±0.5***
Spleen	-	-	-	7.0±0.4	**3.9±0.9***	**2.1±0.2***	1.5±0.1	0.6±0.2	†

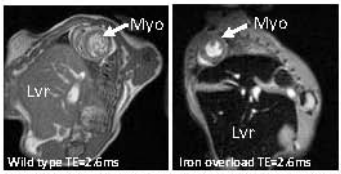

Figure1. Control (L) and iron overload (R) T2 weighted images

C20

Assessment of radiation damaged mouse lungs using perfluorohexane liquid MRI

Alexandr Khrapichev, CR-UK/MRC Oxford Institute for Radiation Oncology, UK

Imaging plays a major role in assessment of pulmonary diseases and a broad spectrum of imaging techniques are available. The main workhorse modality is still computed tomography (CT), which allows fast assessment of the lung parenchyma and surrounding structures. However, the soft tissue contrast and direct functional information that can be obtained is limited. MRI of the lung is difficult owing to the low proton density of the tissue resulting in low signal intensity on conventional 1H scans. The use of hyperpolarized 3He or 129Xe is a viable, but expensive method of lung MRI. As an alternative method, we investigated the possibility of mouse lung imaging using 19F MRI. Strong MR signal of 19F (83% of 1H) combined with high concentration of 19F in liquid makes perfluorohexane ideal for MRI. Biocompatibility and very high oxygen solubility of perfluorohexane (41mL O2/100g), makes "fluid-breathing" and, therefore, in vivo experiments a possibility. Additionally, the absence of fluorine in the body results in bright lungs with no background signal [1].
As an application of 19F MRI, we have chosen a mouse model of lung radiation damage. For the pilot study, 16 female CBA mice were anaesthetized with isoflurane and the left lung irradiated with a 20Gy dose (SARRP, Xtrahl Ltd., UK). Starting at week 6, one animal was sacrificed each week for ex vivo MRI. Each mouse was tracheotomized, and air in the lungs replaced with perfluorohexane (C6F14).
MR images were acquired with standard 3D gradient echo sequences in a 7T spectrometer (Agilent Inc., USA). Throughout the time-course, mice were observed for clinical signs, lung performance measured by plethysmography and behavior monitored.
The typical SNR of 19F MRI is broadly similar to that obtained from 129Xe hyperpolarization experiments [2]. However, higher image resolution allows qualitative analysis of disease progress: the left lung post-irradiation (Fig 1b) appears smaller and less intense than naïve mouse lung (Fig 1a), illustrating subtle anatomical changes invisible on standard 1H MR images. Quantitative volumetric analysis highlights early changes in relative lung volume (Fig 2a), whilst the mean signal intensity of the irradiated lung (Fig 2b) reveals a highly significant reduction, indicating lung damage starting long before clinical signs begin to appear.
The ability to monitor lung damage from early stages could be an important diagnostic tool. 19F based perfluorohexane imaging gives bright and detailed lung images, which allow visualization of structures not apparent on proton MRI. This approach is more easily and cheaply implemented than hyperpolarized gas set-ups and is immediately applicable in a range of pre-clinical work.
This work was supported by a Cancer Research UK core grant to Nicola Sibson (C5255/A12678).

(1) Weigel JK, Steinmann D, Emerich P, Stahl CA, v Elverfeldt D, Guttmann J. "High-resolution three-dimensional 19F-magnetic resonance imaging of rat lung in situ: evaluation of airway strain in the perfluorocarbon-filled lung". Physiol Meas 2011 32(2): 251-62.
(2) Freeman MS, Cleveland ZI, Qi Y, Driehuys B "Enabling hyperpolarized 129Xe MR spectroscopy and imaging of pulmonary gas transfer to the red blood cells in transgenic mice expressing human hemoglobin". Magn Reson Med 2013 70(5): 1192-99.

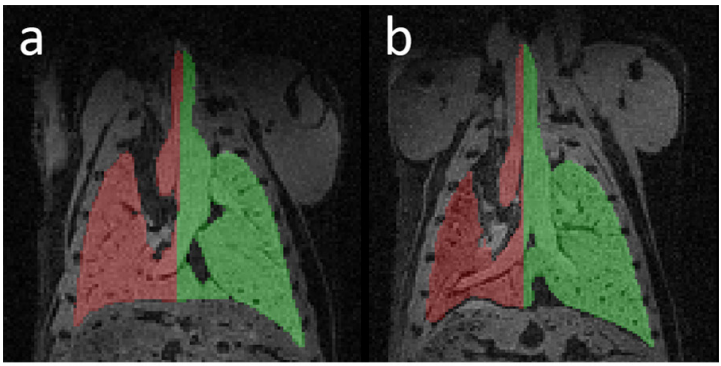

Fig 1. Superposition of 3D ^{1}H MR body images (gray scale) with ^{19}F MR lung images (coloured: left - red, right - green) of a naïve mouse (left) and a mouse 20 weeks

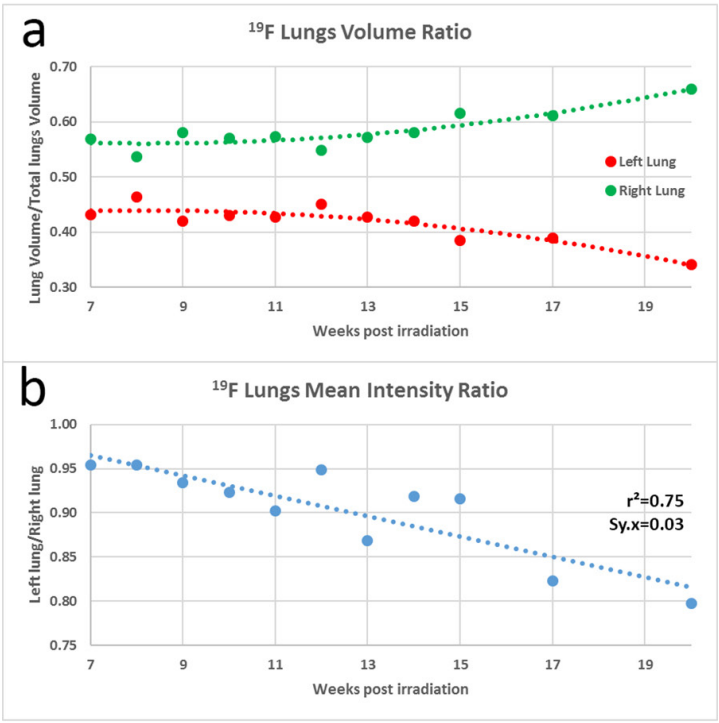

Fig 2. Lung volume ratio (top) and lung mean intensity ratio (bottom) post irradiation.

C21

Non-Invasively Assessing the Microstructural Changes in Tissue Post-Fixation using VERDICT MRI.

Ben Jordan, University College London, UK

Introduction

The purpose of this study was to evaluate the ability of the VERDICT MRI model of compartmental diffusion to quantify tumour microstructure and use it to assess the effects of tissue fixation. Previously it has been demonstrated that the VERDICT model can be successfully used in-vivo to access histologic features such as cell size, vascular volume fraction, intra- and extracellular volume fractions and microvascular pseudo-diffusivity1. However, the gold standard cell diameter values attained through histological analysis were on average 12.3% smaller than the VERDICT measurements. This discrepancy was attributed to the shrinkage of cells during the fixation process. In this study both in vivo and ex-vivo data acquired from the same subjects are compared to ascertain whether the expected cell shrinkage can be detected in the VERDICT estimate of cell size.

Methods and Materials

LS174T cells were injected subcutaneously into 5 female MF1 nu/nu mice (106 cells per animal)2. Animals were scanned on a 9.4T Varian 20cm horizontal bore scanner (Varian Inc. Palo Alto, CA, USA) with a maximum gradient strength of 400mT/m, and a 39mm birdcage RF coil (Rapid Biomedical, Rimpar, Germany). VERDICT data were acquired using a steady-state respiration-gated PGSE sequence with 46 b-values in total. Gradient separation times Δ = 10, 20, 30, 40ms with duration $\boldsymbol{\delta}$ = 3ms for all Δs and $\boldsymbol{\delta}$ = 10ms for Δ = 30, 40ms. Gradient strength G was stepped from 40 to 400mT/m in steps of 40mT/m for $\boldsymbol{\delta}$ = 3ms and 40, 80, 120mT/m for $\boldsymbol{\delta}$ = 10ms. Perfusion fixation was carried out through the left ventricle using 4% paraformaldehyde (PFA). Model fitting was performed using an iterative optimization scheme in the Camino toolkit3. The "BallSphereStick" model (using the taxonomy of Panagiotaki et al 20124) was fitted to in-vivo data and the 'BallSphere' model was fitted to the ex-vivo data.

Results

The VERDICT model provided an accurate fit to the diffusion data for both in-vivo and ex-vivo samples. The cell-radius parameters produced by the model-fitting are shown. A significant reduction (Wilcoxon rank-sum, p=0.0079) in cell radius was detected between the in-vivo and ex-vivo datasets, in agreement with previous findings. The measured decrease in cell size was supported by a significant (p=0.0079) decrease in the intra-cellular volume fraction and an increase in the extracellular volume fraction.

Discussion

We measured a significant decrease in cell radius and intracellular volume fraction in a subcutaneous colorectal tumour model, caused by perfusion fixation. This

decrease was mirrored by a decrease in the intracellular volume, and an increase in the extracellular volume. Such changes are consistent with cell shrinkage, potentially caused by the tissue fixation process. A potential limitation of this method was the slight variation in models used to represent in-vivo and ex-vivo data.

Conclusion

This study aimed to evaluate whether a decrease in tumour cell size caused by chemical fixation could be measured using VERDICT MRI. The initial findings of this study show that VERDICT MRI may indeed be able to access both useful prognostic measures in-vivo and important histologic measures in ex-vivo samples. Future in-silico work will be used to help further validate these findings.

B. Jordan[1], T. Roberts[1], A. D'Esposito[1], J. Connell[1], A. Ianus[2], E. Panagiotaki[2], D. C. Alexander[2], M. F. Lythgoe[1], S. Walker-Samuel[1]

[1] Centre for Advanced Biomedical Imaging, Division of Medicine, University College London,
London, UK.

[2] Centre for Medical Image Computing, University College London, London, UK.

References

1. Panagiotaki et al, Cancer Research 2014. 2. Folerin et al, Microvasc Research (2010). 3. Cook et al, ISMRM

(2006). 4. Panagiotaki et al, Neuroimage (2012).

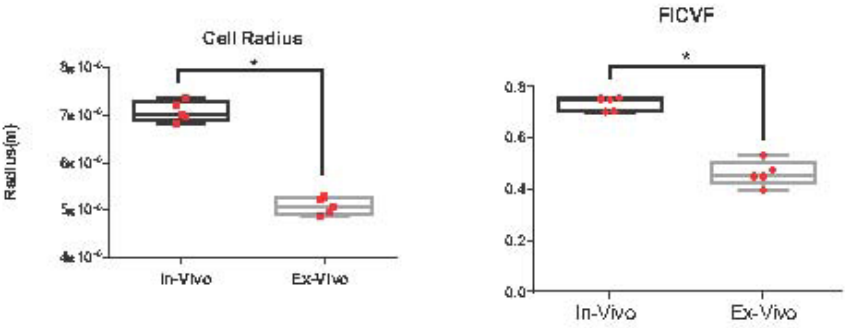

Photography Competition

PHYSIOLOGY IN OUR TIME

Send us your images of physiology for your change to win a cash prize of £300

We are inviting you all to take part in The Physiological Society's photography competition *Physiology in our time*.

The Society has long documented our Members, their labs, and their universities through the eye of the camera lens and we ask you to join us in documenting today's landscape.

Participants can take either a single shot, or a number of shots captioned with at least **200 words** detailing how the images represent physiological research or eminent physiologists in our time. Images could include photos of supervisors, groups, equipment, lab space, university grounds to name a few examples.

Entries will be judged by Members of our History and Archives Committee and photography professionals.

Deadline: Friday 23 September 2016

Find some example shots, and full details, including terms and conditions please visit our website:

www.physoc.org/physiology-in-our-time

The Physiological Society

The science of life

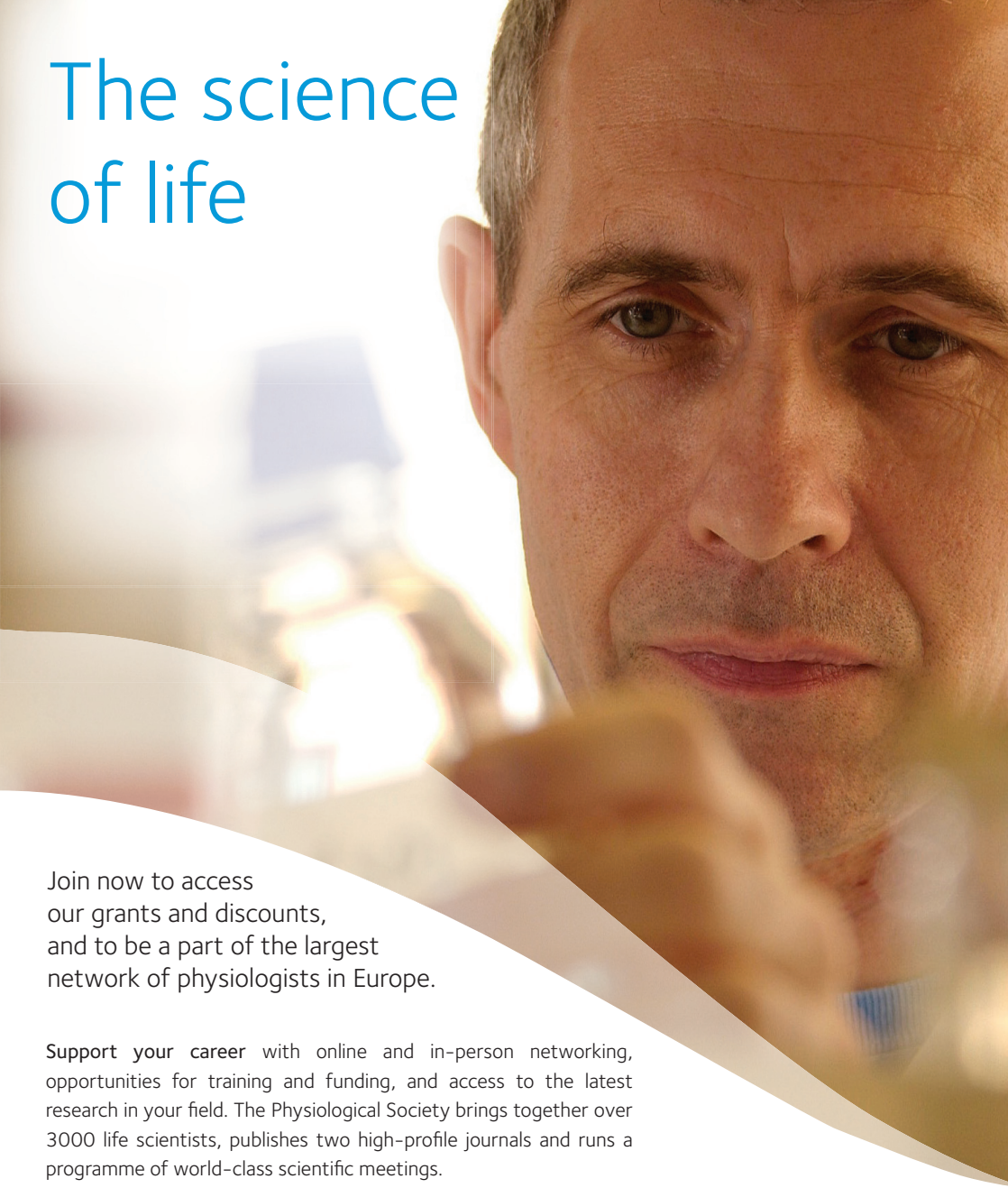

Join now to access
our grants and discounts,
and to be a part of the largest
network of physiologists in Europe.

Support your career with online and in-person networking, opportunities for training and funding, and access to the latest research in your field. The Physiological Society brings together over 3000 life scientists, publishes two high-profile journals and runs a programme of world-class scientific meetings.

Support physiology as a discipline. The Physiological Society works to raise the profile of scientific research and education with policy makers and the general public.

For more information on membership options visit **www.physoc.org**

The Physiological Society